

96 sh.

**THE FREE VIBRATION ANALYSIS OF MULTI
DISC-SHAFT SYSTEMS**

119645

**A Thesis Submitted to the Graduate School of Natural and Applied Sciences of
Dokuz Eylül University In Partial Fulfillment of the Requirements for
The Degree of Master of Science in
Mechanical Engineering,
Machine Theory and Dynamics Program**

**T.C. YÜKSEKÖĞRETİM KURULU
DOKÜMANTASYON MERKEZİ**

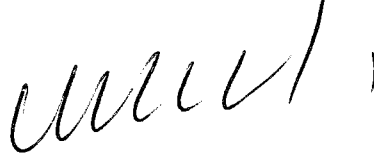
by
Murat AKDAĞ

**December, 2002
İZMİR**

119645

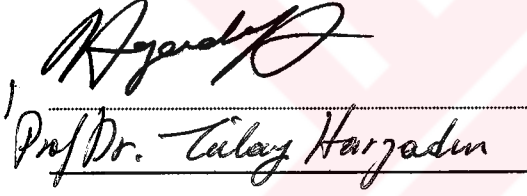
M.Sc THESIS EXAMINATION RESULT FORM

We certify that we have read this thesis and “**The Free Vibration Analysis of Multi Disc-Shaft Systems** ” completed by **Murat AKDAĞ** under supervision of **Prof. Dr. Mustafa SABUNCU** and that in our opinion it is fully adequate, in scope and in quality, as a thesis for the degree of Master of Science.

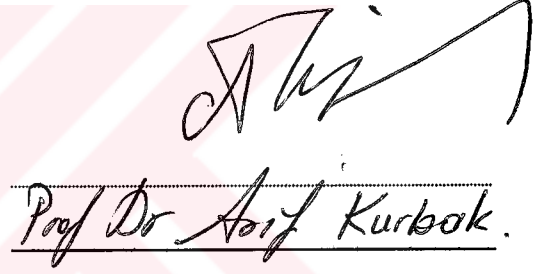


Prof. Dr. Mustafa SABUNCU

Supervisor



(Committee Member)



(Committee Member)

Approved by the
Graduate School of Natural and Applied Sciences



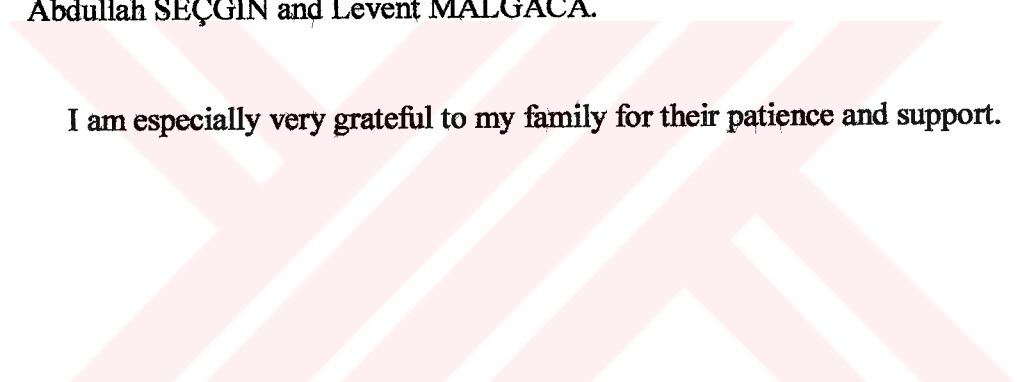
Prof. Dr. Cahit HELVACI
Director

ACKNOWLEDGMENTS

I would like to thank to my supervisor Prof. Dr. Mustafa SABUNCU, my advisor whose guidance, constructive suggestions and continued interest were vital to the completion of this work.

My thanks also extend to my friends at the department of Mechanical Engineering, especially to Research Assistant Zeki KIRAL, Gürkan ŞAKAR, Binnur GÖREN, Abdullah SEÇGİN and Levent MALGACA.

I am especially very grateful to my family for their patience and support.



ABSTRACT

In this study, effects of the mass properties and positions of one or more discs having shafts with variable cross sections on free vibrations have been investigated. Torsional vibration analysis of multi disc-shaft systems have been carried out by using the Transfer Matrix and the Finite Element Method. To show the accuracy of the programs that are developed, the obtained results are compared with the available results of other investigators in the existing literature. Effects of the number of discs and their positions on the shaft and the variation of cross section of the shaft on the natural frequencies have been shown in graphics. In addition, the results obtained by using two different methods are compared and very good agreement is found.

The MATLAB 5.1 and Visual BASIC computer programs was used in this study.

ÖZET

Bu çalışmada bir mil üzerinde bulunan bir ve birden fazla diskin kütleli özellikleri ve konumları ile milin kesit değişimlerinin serbest titreşimlere olan etkileri incelenmiştir. Çoklu disk-mil sistemlerinin burulma titreşimlerinin analizi Transfer Matrisi ve Sonlu Elemanlar Metodu kullanılarak yapılmıştır. Geliştirilen programdan elde edilen sonuçların doğruluğu, literatürde yer alan bazı sonuçlarla karşılaştırılarak görülmüştür. Disklerin sayılarının, mil üzerindeki konumlarının ve mildeki kesit farklılıklarının sistemin doğal frekansları üzerindeki etkileri grafikler halinde gösterilmiştir. Ayrıca her iki metottan elde edilen sonuçlar da birbirleriyle karşılaştırılmış ve büyük bir uyum gözlenmiştir.

Bu çalışmada MATLAB 5.1 ve Visual BASIC bilgisayar programları kullanılmıştır.

CONTENTS

| | |
|-----------------|-----|
| Contents | IV |
| List of Tables | VI |
| List of Figures | VII |
| Nomenclature | XI |

Chapter One INTRODUCTION

| | |
|------------------|---|
| 1.1 Introduction | 1 |
|------------------|---|

Chapter Two NUMERICAL METHODS

| | |
|---|----|
| 2.1 The Finite Element Method | 3 |
| 2.1.1 What is the Finite Element Method? | 3 |
| 2.1.2 How the Method Works | 6 |
| 2.1.3 Range of Applications | 10 |
| 2.2 The Transfer Matrix Method | 12 |
| 2.2.1 State Vector | 12 |
| 2.2.2 Coordinate System and Sign Convention | 14 |

| | |
|--|----|
| 2.2.3 Transfer Matrix | 15 |
| 2.2.4 Transfer Matrix for a Torsional System | 17 |

Chapter Three

THEORETICAL ANALYSIS

| | |
|---|----|
| 3.1 Introduction | 20 |
| 3.2 Determination of the Area and second Moment of Area for a Shaft Finite Element | 22 |
| 3.3 Determination of Deflections of a Finite Element | 24 |
| 3.3.1 Evaluation of the Element Elastic Stiffness Matrix | 25 |
| 3.3.2 Evaluation of the Mass Matrix | 26 |
| 3.4 Evaluation of the Transfer Matrix Method | 26 |

Chapter Four

RESULTS AND DISCUSSION

| | |
|-------------------|----|
| References | 54 |
| Appendix | 56 |

LIST OF TABLES

| | | |
|-----------|---|----|
| Table 4.1 | Comparison with Finite Element Method and Transfer Matrix Method..... | 35 |
| Table 4.2 | Comparison of the first natural frequency results of the clamped support from left and right which can be seen in Fig. 4.27 and Fig. 4.29..... | 51 |



LIST OF FIGURES

| | | |
|----------------|---|----|
| Figure 2.1 | Finite difference and finite element discretizations of a turbine blade profile. (a) Typical finite difference model. (b) Typical finite element model..... | 5 |
| Figure 2.2 | Spring-mass system..... | 12 |
| Figure 2.3 | Torsional system..... | 13 |
| Figure 2.4 | Sign convention..... | 14 |
| Figure 2.5 | Vector symbols..... | 14 |
| Figure 2.6 | Free-body of spring and mass..... | 15 |
| Figure 2.7 (a) | Massless shaft with disks..... | 17 |
| Figure 2.7 (b) | free-body diagram of shaft..... | 18 |
| Figure 2.7 (c) | free-body diagram of disk..... | 18 |
| Figure 3.1 | Uniform shaft..... | 21 |
| Figure 3.2 | Linear (Tapered) shaft..... | 21 |
| Figure 3.3 | Parabolic (Concave) shaft..... | 21 |
| Figure 3.4 | Parabolic (Convex) shaft..... | 22 |
| Figure 3.5 | Discretizations of the shaft..... | 23 |
| Figure 3.6 | Average diameter of a shaft element..... | 23 |
| Figure 3.7 | Shaft elements having average diameters..... | 24 |
| Figure 3.8 | A Uniform Torsion Element..... | 24 |
| Figure 3.9 | Shaft-Disk System..... | 27 |
| Figure 4.1 | Idealized machine shaft..... | 34 |
| Figure 4.2 | Two disks-shaft system with, free-free support condition. $I=3.389 \text{ kg.m}^2 \quad l=0.5 \text{ m}.$ | 35 |

| | | |
|-------------|---|----|
| Figure 4.3 | Comparison of the results of the Finite Element and the Transfer Matrix Methods with respect to torsional stiffness on the natural frequency of vibration for a multi disc-shaft system (Fig. 4.2). $n=2, I=3.389 \text{ kg.m}^2, l=0.5 \text{ m}$ | 36 |
| Figure 4.4 | Comparison of the results of the Finite Element and the Transfer Matrix Methods with respect to disc inertia on the natural frequency of vibration for a multi disc-shaft system (Fig. 4.2) $n=2, I=3.389 \text{ kg.m}^2, l=0.5 \text{ m}$ | 36 |
| Figure 4.5 | The effects of torsional stiffness and the number of discs on the first natural frequency of vibration $I=3.38937 \text{ kg.m}^2$ | 37 |
| Figure 4.6 | The effects of torsional stiffness and the number of discs on the first natural frequency of vibration $k=112979.2 \text{ Nm/rad}$ | 38 |
| Figure 4.7 | The multi disk-shaft system that having disk with free-free support condition. $l=1 \text{ m}, d=0.05 \text{ m}$ | 39 |
| Figure 4.8 | The effects of the distance of the middle disk from the first disk and the disks inertias on the second natural frequency of vibration..... | 39 |
| Figure 4.9 | The effects of the distance of the middle disk from the first disk and the disks inertias on the third natural frequency of vibration..... | 40 |
| Figure 4.10 | The multi disk-shaft system having two disk with clamped-free support condition. $l=1 \text{ m}, d=0.05 \text{ m}$ | 40 |
| Figure 4.11 | The effects of the distance of the middle disk from the clamped support and the disks inertias on the first natural frequency of vibration..... | 41 |
| Figure 4.12 | The effects of the distance of the middle disk from the clamped support and the disks inertias on the second natural frequency..... | 41 |
| Figure 4.13 | The single disk-shaft system with clamped- clamped support condition. $l=1 \text{ m}, d=0.05 \text{ m}$ | 42 |
| Figure 4.14 | The effects of the distance of the disk from the left clamped support and the disk inertia on the first natural frequency..... | 42 |

| | | |
|-------------|--|----|
| Figure 4.15 | The effects of the distance of the disk from the left clamped support and the disk inertia on the second natural frequency..... | 43 |
| Figure 4.16 | The multi disk-shaft system having four disk with free- free support condition. $l=1$ m, $d=0.05$ m..... | 43 |
| Figure 4.17 | The effects of the distance of the middle two disk from the left and right discs and the disks inertias on the second natural frequency.... | 44 |
| Figure 4.18 | The effects of the distance of the middle two disk from the left and right discs and the disks inertias on the third natural frequency..... | 44 |
| Figure 4.19 | The multi disk-shaft system having three disk with clamped-free support condition. $l=1$ m, $d=0.05$ m..... | 45 |
| Figure 4.20 | The effects of the distance of the middle two disc from the left clamped support and the right disc and the discs inertias on the first natural frequency of vibration..... | 45 |
| Figure 4.21 | The effects of the distance of the middle two disc from the left clamped support and the right disc and the discs inertias on the second natural frequency of vibration..... | 46 |
| Figure 4.22 | The multi disk-shaft system having two disk with clamped-clamped support condition $l=1$ m, $d=0.05$ m..... | 46 |
| Figure 4.23 | The effects of the distance of the middle two disk from the left and right clamped support and the discs inertias on the first natural frequency of vibration..... | 47 |
| Figure 4.24 | The effects of the distance of the middle two disk from the left and right clamped support and the discs inertias on the second natural frequency of vibration..... | 47 |
| Figure 4.25 | The multi disc-shaft system having two disk and tapered shaft with free-free support condition $l=1$ m $d_{initial}=0.05$ m $d_{end}=0.15$ m..... | 48 |
| Figure 4.26 | The effects of changing initial diameter and the inertia of the disks on the second natural frequency of vibration for the system shown in Fig. 4.25..... | 48 |

| | | |
|-------------|--|----|
| Figure 4.27 | The disc-shaft system having a disk and tapered shaft with clamped-free support condition. $l=1$ m $d_{\text{initial}}=0.05$ m $d_{\text{end}}=0.15$ m..... | 49 |
| Figure 4.28 | The effects of changing initial diameter of tapered shaft and the inertia of the disk on the first natural frequency of vibration for the system shown in Fig. 4.27..... | 49 |
| Figure 4.29 | The disc-shaft system having a disk and tapered shaft with free-clamped support condition. $l=1$ m $d_{\text{initial}}=0.05$ m $d_{\text{end}}=0.15$ m..... | 50 |
| Figure 4.30 | The effects of changing initial diameter of tapered shaft and the inertia of the disk on the first natural frequency of vibration for the system shown in Fig. 4.29..... | 50 |
| Figure 4.31 | The multi disk-shaft systems having two discs and (a) tapered, (b) concave, (c) convex shaft with free-free support conditions..... | 51 |
| Figure 4.32 | The effects of increasing the first diameter of convex, tapered and concave shaft on the first natural frequency for the systems shown in Fig. 4.31..... | 52 |
| Figure 4.33 | The effects of increasing the length of convex, tapered and concave shaft on the first natural frequency for the systems shown in Fig. 4.31..... | 52 |
| Figure 4.34 | The effects of increasing the inertia of the discs on convex, tapered and concave shaft on the first natural frequency for the systems shown in Fig. 4.31..... | 53 |

NOMENCLATURE

| | |
|----------------------|--|
| A | Cross-sectional area |
| a | distance of disk from the left hand side |
| A(x) | Cross-section area of the shaft |
| d(x) | Diameter of the shaft |
| d ₁ | Diameter free-end of the shaft |
| d _{average} | Average diameter of the shaft |
| d _o | Diameter at root of the shaft |
| e | Finite element length |
| E | Young's modulus |
| F | Field transfer matrix |
| G | Shear modulus |
| I | Mass moment of inertia |
| I _p | Polar moment of inertia |
| J | Polar second moment of area |
| k | Torsional stiffness |
| L, l | Length |
| M | Moment |
| n | Number of disk |
| N | Normal force |
| P | Point transfer matrix |
| T | Kinetic energy |
| T | Torque |
| V | Strain energy |
| V | Shear force |

| | |
|----------|---|
| x | Displacement |
| z | State vector |
| $[k]$ | Stiffness matrix of the elemental finite element |
| $[K]$ | Total elastic stiffness matrix |
| $[M]$ | Total mass (inertia) matrix |
| $[m]$ | Mass (inertia) matrix of the elemental finite element |
| ω | Natural circular frequency |
| ρ | Mass density |
| ν | Poisson ratio |
| ϕ | Rotation about x axis |



CHAPTER ONE

INTRODUCTION

1.1 Introduction

Multi disk-shaft systems are employed in various machines used in industry. Various working parts in those machines can be reduced to multi disc-shaft systems. For instance, in a reciprocating machine crank-shaft, connecting rod and piston can be modeled as an idealized shaft and disk system. Here the disk stands for the connecting rod and piston, the shaft stands for the crank shaft. Ship propellers, gear boxes, turbines, helicopter propellers and lathes are some of the examples to those machines. The number of examples can be increased.

Torsional stresses entail the most important subject for the multi disc-shaft systems because they are known as the most dangerous stresses on rotating shafts. Therefore torsional vibration analysis of rotating shafts is inevitable in the design stage. The natural frequencies of these systems must be known and taken into consideration for the working frequency.

The vibration analysis of multi disc-shaft systems have been carried out by analytical and numerical methods. The analytical method solutions of multi disc-shaft systems take a long time and therefore the chance of making mistakes increases. For this reason, numerical methods that give sensitive results are commonly used. The fast advancement of computers have made the use of numerical methods easy.

The works of [1] Pestel and Leckie are the main references on how to solve the multi disc-shaft systems using transfer matrix method. They give various samples about these systems.

[3] Özgüven have calculated the percentage errors in order to find the critical velocities of continuous disc-shaft systems taking into consideration the disc and shaft mass and the shaft length.

[8] Köser and Pasin have investigated the torsional vibrations of forced shaft systems. They have assumed that the shaft is a continuous element and the system has various inertia characteristics. The problem then reduced to a non-linear boundary value problem and the solution has been made by the perturbation method in their study.

[10] Kaneko, Momoo and Okada have studied the torsional vibrations of turbin blade-disc-shaft systems by the Finite Element and the Transfer Matrix Methods. While blade-disc systems have been calculated by the Finite Element Method, blade-disc-shaft systems have been calculated by the Transfer Matrix Method.

[11] Kato, Ota and Nakamura have examined the torsional vibrations of elastic shafts carrying the rotor when it is passing through critical velocities.

CHAPTER TWO

NUMERICAL METHODS

2.1 The Finite Element Method

2.1.1 What is the Finite Element Method?

The finite element method is a numerical analysis technique for obtaining approximate solutions to a wide variety of engineering problems. Although it was originally developed to study the stresses in complex airframe structures, it has since been extended and applied to the broad field of continuum mechanics. On account of its diversity and flexibility as an analysis tool, it is receiving much attention in engineering schools and in industry.

In complex engineering problems today, we find that it is necessary to obtain approximate numerical solutions to problems rather than exact closed-form solutions. For example, we may want to calculate the load capacity of a plate that has several stiffeners and odd-shaped holes, the concentration of pollutants during non-uniform atmospheric conditions or the rate of fluid flow through a passage of arbitrary shape. Without too much effort, we can write down the governing equations and boundary conditions for these problems, but we can easily see that no simple analytical solution can be found. The difficulty in these three examples give above, lies in the fact that either the geometry or some other feature of the problem is irregular or "arbitrary." Analytical solutions to problems of this type seldom exist; yet these are the kinds of problems that engineers and scientists are called upon to solve.

The resourcefulness of the analyst usually comes to the rescue and provides several alternatives to overcome this dilemma. One possibility is to make simplifying assumptions-to ignore the difficulties and reduce the problem to one that can be handled. Sometimes this procedure works; but, more often than not, it leads to serious inaccuracies or wrong answers. Now that large-scale digital computers are widely available, a more viable alternative is to retain the complexities of the problem and try to find an approximate numerical solution.

Several approximate numerical analysis methods have evolved over the years-one of the most commonly used methods is the general finite difference scheme. The familiar finite difference model of a problem gives a point wise approximation to the governing equations. This model (formed by writing difference equations for an array of grid points) is improved as more points are used. With finite difference techniques we can treat some fairly difficult problems; but, for example, when we encounter irregular geometries or an unusual specification of boundary conditions, we find that finite difference techniques become hard to use.

In addition to the finite difference method, another, more recent numerical method (known as the "Finite Element Method") has emerged. Unlike the finite difference method, which envisions the solution region as an array of grid points, the finite element method envisions the solution region as built up of many small, interconnected sub-regions or elements. A finite element model of a problem gives a piece-wise approximation to the governing equations. The basic premise of the finite element method is that a solution region can be analytically modeled or approximated by replacing it with an assemblage of discrete elements. Since these elements can be put together in a variety of ways, they can be used to represent exceedingly complex shapes.

As an example of how a finite difference model and a finite element model might be used to represent a complex geometrical shape, consider the turbine blade cross section in

Figure 2.1. For this blade we may want to find the distribution of displacements and stresses for a given force loading or the distribution of temperature for a given thermal loading. The interior coolant passage of the blade, along with its exterior shape, gives it a non-simple geometry.

A uniform finite difference mesh would reasonably cover the blade (the solution region), but the boundaries must be approximated by a series of horizontal and vertical lines (or "stair steps"). On the other hand, the finite element model (using the simplest

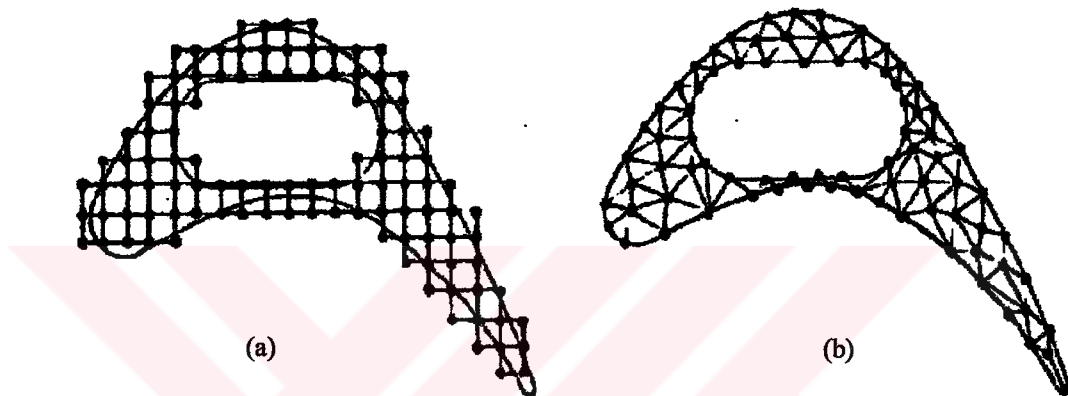


Figure 2.1 Finite difference and finite element discretizations of a turbine blade profile. (a) Typical finite difference model. (b) Typical finite element model.

two-dimensional element- the triangle) gives a better approximation to the region and requires fewer nodes. Also, a better approximation to the boundary shape results because the curved boundary is represented by a series of straight lines. This example is not intended to suggest that finite element models are decidedly better than finite difference models for all problems. The only purpose of the example is to demonstrate that the finite element method is particularly well suited for problems with complex geometries.

2.1.2 How the Method Works

We have been alluding to the essence of the finite element method, but now we shall discuss it in greater detail. In a continuum problem of any dimension the field variable (whether it is pressure, temperature, displacement, stress or some other quantity) possesses infinitely many values because it is a function of each generic point in the body or solution region. Consequently, the problem is one with an infinite number of unknowns. The finite element discretization procedures reduce the problem to one of a finite number of unknowns by dividing the solution region into elements and by expressing the unknown field variable in terms of assumed approximating functions within each element. The approximating functions (sometimes called interpolation line functions) are defined in terms of the values of the field variables at specified points called nodes or nodal points. Nodes usually lie on the element boundaries where adjacent elements are considered to be connected. In addition to boundary nodes, an element may also have a few interior nodes. The nodal values of the field variable and the interpolation functions for the elements completely define the behavior of the field variable within the elements. For the finite element representation of a problem the nodal values of the field variable become the new unknowns. Once these unknowns are found, the interpolation functions define the field variable throughout the assemblage of elements.

Clearly, the nature of the solution and the degree of approximation depend not only on the size and number of the elements used, but also on the interpolation functions selected. As one would expect, we cannot choose functions arbitrarily, because certain compatibility conditions should be satisfied. Often functions are chosen so that the field variable or its derivatives are continuous across adjoining element boundaries.

Thus far we have briefly discussed the concept of modeling an arbitrarily shaped solution region with an assemblage of discrete elements and we have pointed out that interpolation functions must be defined for each element. We have not yet mentioned,

however, an important feature of the finite element method that sets it apart from other approximate numerical methods. This feature is the ability to formulate solutions for individual elements before putting them together to represent the entire problem. This means, for example, that if we are treating a problem in stress analysis, we can find the force-displacement or stiffness characteristics of each individual element and then assemble the elements to find the stiffness of the whole structure. In essence, a complex problem reduces to considering a series of greatly simplified problems.

Another advantage of the finite element method is the variety of ways in which one can formulate the properties of individual elements. There are basically four different approaches. The first approach to obtaining element properties is called the direct approach because its origin is traceable to the direct stiffness method of structural analysis. The direct approach also suggests the need for matrix algebra in dealing with the finite element equations.

Element properties obtained by the direct approach can also be determined by the more versatile and more advanced variational approach. The variational approach relies on the calculus of variations and involves extremizing a *functional*. For problems in solid mechanics the functional turns out to be the potential energy, the complementary potential energy or some derivative of these, such as the Reissner variational principle. Knowledge of the variational approach is necessary to work beyond the introductory level and to extend the finite element method to a wide variety of engineering problems. Whereas the direct approach can be used to formulate element properties for only the simplest element shapes, the variational approach can be employed for both simple and sophisticated element shapes.

A third and even more versatile approach to deriving element properties has its basis entirely in mathematics and is known as the weighted residuals approach. The weighted residuals approach begins with the governing equations of the problem and proceeds

without relying on a functional or a variational statement. This approach is advantageous because it thereby becomes possible to extend the finite element method to problems where no functional is available. For some problems we do not have a functional-either because one may not have been discovered or because one does not exist.

A fourth approach relies on the balance of thermal and/or mechanical energy of a system. The energy balance approach (like the weighted residuals approach) requires no variational statement and hence broadens considerably the range of possible applications of the finite element method.

Regardless of the approach used to find the element properties, the solution of a continuum problem by the finite element method always follows an orderly step-by-step process.

1. Discretize the Continuum. The first step is to divide the continuum or solution region into elements. In the example of Figure 2.1 the turbine blade has been divided into triangular elements that might be used to find the temperature distribution or stress distribution in the blade. A variety of element shapes may be used and with care, different element shapes may be employed in the same solution region. Indeed, when analyzing an elastic structure that has different types of components such as plates and beams, it is not only desirable but also necessary to use different types of elements in the same solution. Although the number and the type of elements to be used in a given problem are matters of engineering judgment, the analyst can rely on the experience of others for guidelines.

2. Select interpolation functions. The next step is to assign nodes to each element and then choose the type of interpolation function to represent the variation of the field variable over the element. The field variable may be a scalar, a vector or a higher-order tensor. Often, although not always, polynomials are selected as interpolation functions for the field variable because they are easy to integrate and differentiate. The degree of the

polynomial chosen depends on the number of nodes assigned to the element, the nature and number of unknowns at each node and certain continuity requirements imposed at the nodes and along the element boundaries. The magnitude of the field variable as well as the magnitude of its derivatives may be the unknowns at the nodes.

3. Find the element properties. Once the finite element model has been established (that is, once the elements and their interpolation functions have been selected), we are ready to determine the matrix equations expressing the properties of the individual elements. For this task we may use one of the four approaches just mentioned: the direct approach, the variational approach, the weighted residual approach or the energy balance approach. The variational approach is often the most convenient, but for any application the approach used depends entirely on the nature of the problem.

4. Assemble the element properties to obtain the system equations. To find the properties of the overall system modeled by the network of elements we must “assemble” all the element properties. In other words, we must combine the matrix equations expressing the behavior of the elements and form the matrix equations expressing the behavior of the entire solution region or system. The matrix equations for the system have the same form as the equations for an individual element except that they contain many more terms because they include all nodes.

The basis for the assembly procedure stems from the fact that at a node, where elements are interconnected, the value of the field variable is the same for each element sharing that node. Assembly of the element equations is a routine matter in the finite element analysis and is usually done by a digital computer.

Before the system equations are ready for solution they must be modified to account for the boundary conditions of the problem.

5. Solve the system equations. The assembly process of the preceding step gives a set of simultaneous equations that we can solve to obtain the unknown nodal values of the field variable.

6. Make additional computations if desired. Sometimes we may want to use the solution of the system equations to calculate other important parameters. For example, in a fluid mechanics problem such as the lubrication problem, the solution of the system equations gives the pressure distribution within the system. From the nodal values of the pressure we may then calculate velocity distributions and flows or perhaps shear stresses if these are desired.

2.1.3 Range of Applications

Applications of the finite element method can be divided into three categories, depending on the nature of the problem to be solved. In the first category all the problems are known as *equilibrium problems* or time-independent problems. The majority of applications of the finite element method fall into this category. For the solution of equilibrium problems in the solid mechanics area we need to find the displacement distribution or the stress distribution or perhaps the temperature distribution for a given mechanical or thermal loading. Similarly, for the solution of equilibrium problems in fluid mechanics, we need to find pressure, velocity, temperature and sometimes concentration distributions under steady-state conditions.

In the second category so-called eigenvalue problems, are the problems of solid and fluid mechanics. These are steady-state problems whose solution often requires the determination of natural frequencies and modes of vibration of solids and fluid. Examples of eigenvalue problems involving both solid and fluid mechanics appear in civil engineering when the interaction of lakes and dams is considered and in aerospace

engineering when the surge of liquid fuels in flexible tanks is involved. Another class of eigenvalue problems includes the stability of structures and the stability of laminar flows.

In the third category is the multitude of time-dependent or propagation problems of continuum mechanics. This category is composed of the problems that result when the time dimension is added to the problems of the first two categories.

Just about every branch of engineering is a potential user of the finite element method. But the mere fact that this method can be used to solve a particular problem does not mean that it is the most practical solution technique. Often several attractive techniques are available to solve a given problem. Each technique has its relative merits and no technique enjoys the lofty distinction of being “the best” for all problems. Consequently, when a designer or analyst has a continuum problem to solve, his first major step is to decide which method to use. This involves a study of the alternative methods of solution, the availability of computer facilities and computer packages and most important of all, the amount of time and money that can be spent to obtain a solution.

The range of possible applications of the finite element method extends to all engineering disciplines, but civil and aerospace engineers concerned with stress analysis are the most frequent users of the method. Major aircraft companies and other organizations involved in the design of structures have developed elaborate finite element computer programs.

2.2 The Transfer Matrix Method

2.2.1 State Vector

The state vector at a point i of elastic systems is a column vector, the components of which are the displacements of the point i and the corresponding internal forces. In the simple case of a spring-mass system (Figure 2.2) the displacement of the point i is clearly the linear displacement x_i and the corresponding internal force is the direct force N_i in the spring. For this special case the state vector z_i has the two components x_i , N_i and in matrix notation z_i has the form:

$$z_i = \begin{bmatrix} x_i \\ N_i \end{bmatrix} = \begin{bmatrix} x \\ N \end{bmatrix}_i \quad (2.1)$$

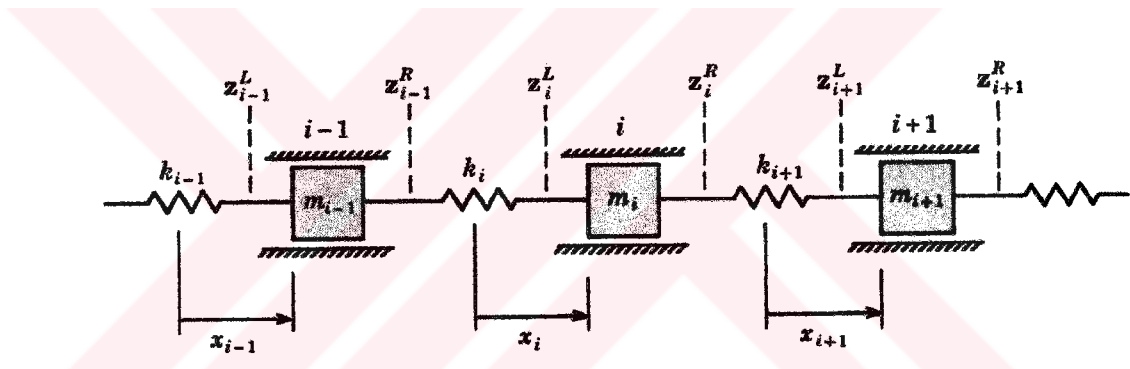


Figure 2.2 Spring-mass system

Analogous to the spring-mass system is the torsion system, consisting of an elastic massless shaft with discs concentrated at different points along its length (Figure 2.3).

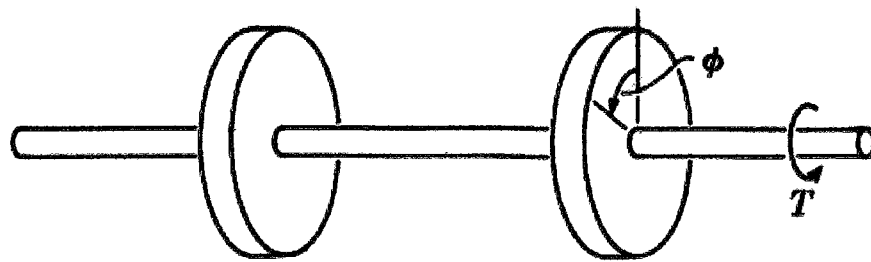


Figure 2.3 Torsional system

The displacement in this case, is the angle of twist ϕ and the corresponding force is the torque T_i . The state vector is then given by:

$$z_i = \begin{bmatrix} \phi \\ T \end{bmatrix}_i \quad (2.2)$$

A more complicated case is that of the straight beam. The displacements at the point i are the deflection w_i and the slope ϕ_i . The internal forces are the shear force V_i corresponding to the displacement w_i and the moment M_i corresponding to the slope ϕ_i . The state vector in this case, therefore, has four components:

$$z_i = \begin{bmatrix} w \\ \phi \\ M \\ V \end{bmatrix}_i \quad (2.3)$$

Notice the order in which the components have been written. The displacements are placed in the upper half of column and the forces in the lower, in such a way that the force and the corresponding displacement (that is, w and V , ϕ and M) are in positions that are mirror images of each other about the center of the column.

2.2.2 Coordinate System and Sign Convention

We shall introduce transfer matrices by referring to the three systems mentioned in the previous section. Before doing so we must define the coordinate system and sign convention. We shall use the right-handed Cartesian coordinate system, the x axis coinciding with the centroidal axis of the elastic body (Figure 2.4). A cut made across the body will expose two faces and the face whose outward normal points in the positive direction of the x axis is known as the positive face, the other being the negative face.

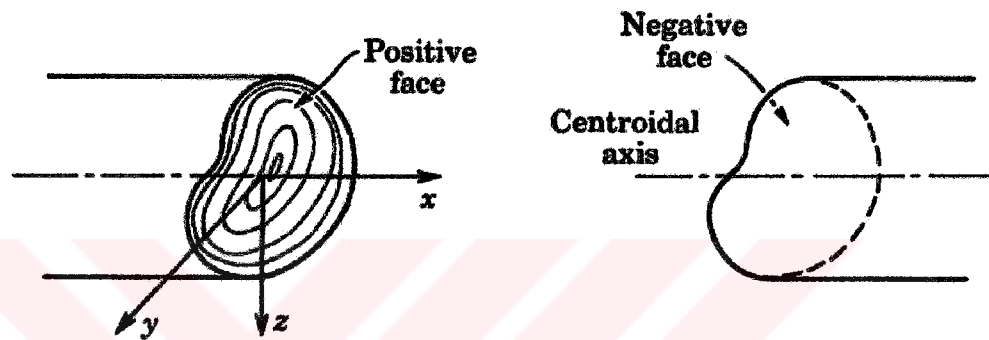


Figure 2.4 Sign convention

Positive displacements coincide with positive direction of the coordinate system and forces are positive if, when acting on the positive (negative) face, their vectors are in the positive (negative) directions. Force vectors are represented by arrows and moment vectors are represented according to the right-hand-screw rule by a double line with an arrowhead (Figure 2.5).



Figure 2.5 Vector symbols

2.2.3 Transfer Matrix

Let us consider a spring-mass system of the type shown in Figure 2.2 which is vibrating with circular frequency ω . The masses m_{i-1} and m_i are connected by a massless spring of stiffness k_i . The state vector just to the right of mass m_i is denoted by z_i^R and the state vector to the left is denoted by z_i^L . If we isolate the spring k_i and use the convention explained above, the positive forces and deflection are as shown in Figure 2.6.a

From the equilibrium of the spring we immediately obtain:

$$N_{i-1}^R = N_i^L \quad (2.4)$$

and from the stiffness property of the spring we have the further relation:

$$N_i^L = N_{i-1}^R = k_i(x_i - x_{i-1}) \quad (2.5)$$

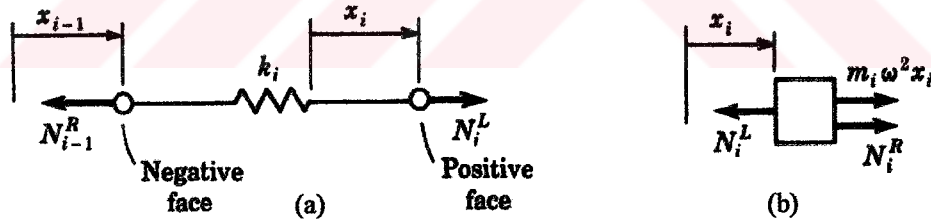


Figure 2.6 Free-body of spring and mass

Rewriting these equations in the form:

$$x_i = x_{i-1} + \frac{N_{i-1}^R}{k_i} \quad N_i^L = (0)x_{i-1} + N_{i-1}^R \quad (2.6)$$

we can then take one more step to express the equation in matrix notation:

$$\begin{bmatrix} x \\ N \end{bmatrix}_i^L = \begin{bmatrix} 1 & \frac{1}{k_i} \\ 0 & 1 \end{bmatrix} \begin{bmatrix} x \\ N \end{bmatrix}_{i-1}^R \quad (2.7)$$

or

$$z_i^L = F_i z_{i-1}^R \quad (2.8)$$

Hence by means of the matrix F_i we have been able to express the state vector z_i^L in terms of the vector z_{i-1}^R . The matrix F_i is known as the field transfer matrix or more simply as the field matrix.

The matrix relation that exists between the state vectors to left and right of mass i can be found by considering the forces (Figure 2.6.b) acting on the mass. The two spring forces are N_i^R and N_i^L and in addition there is the inertia force $m_i \omega^2 x_i$ acting in the positive direction. Since the mass is rigid, the deflections to the left and right of mass m_i are the same, so that:

$$x_i^R = x_i^L \quad (2.9)$$

and from the equilibrium of the forces we have:

$$N_i^R = N_i^L - m_i \omega^2 x_i \quad (2.10)$$

Rewritten in matrix notation, the above equations become:

$$\begin{bmatrix} x \\ N \end{bmatrix}_i^R = \begin{bmatrix} 1 & 0 \\ -m_i \omega^2 & 1 \end{bmatrix} \begin{bmatrix} x \\ N \end{bmatrix}_i^L \quad (2.11)$$

or

$$z_i^R = P_i z_i^L \quad (2.12)$$

Again we have found a matrix relation between two adjacent state vectors. This time, since we are simply transferring over a point, the matrix P_i is known as the point transfer matrix or the point matrix.

2.2.4 Transfer Matrix for a Torsional System

We shall now consider the torsional vibrations of an elastic shaft of circular cross section, with disks attached at discrete points along its axis (Fig. 2.7a). The shaft is elastic and without rotational inertia, and the disks are rigid and have a rotational moment of inertia I_i . The shaft between $i-1$ and i is isolated, the end rotations and torques being indicated in Fig. 2.7b.

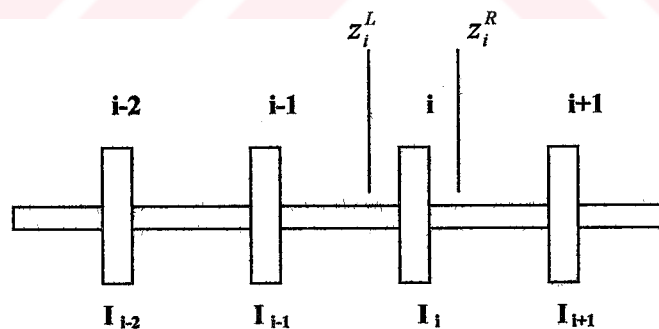


Figure 2.7 (a) Massless shaft with disks

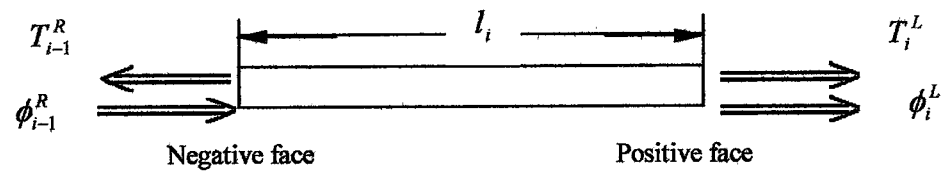


Figure 2.7 (b) free-body diagram of shaft

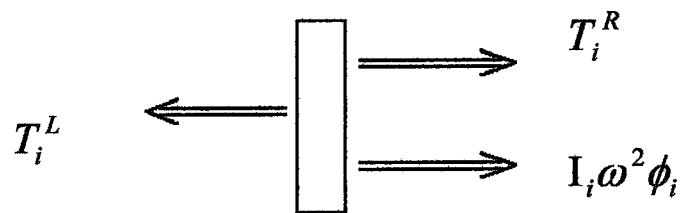


Figure 2.7 (c) free-body diagram of disk

From the equilibrium of the shaft we have

$$T_i^L = T_{i-1}^R \quad (2.13)$$

and from simple strength of materials the relation

$$\phi_i^L - \phi_{i-1}^R = \frac{T_{i-1}^R l_i}{(J_T G)_i} \quad (2.14)$$

where J_T is the polar second moment of area of the shaft and G is the shear modulus of the material.

In matrix notation these two equations become

$$\begin{bmatrix} \phi \\ T \end{bmatrix}_i^L = \begin{bmatrix} 1 & \frac{l}{J_T G} \\ 0 & 1 \end{bmatrix}_i \cdot \begin{bmatrix} \phi \\ T \end{bmatrix}_{i-1}^R \quad (2.15)$$

or

$$z_i^L = F_i z_{i-1}^R \quad (2.16)$$

When relating the state vectors z_i^R and z_i^L on either side of the disk i , we note that the angle of twist remains unchanged, so that $\phi_i^L = \phi_i^R$, but as a result of the inertia torque of the disk there is a discontinuity in the torque. With reference to Fig. 2.7c, the equilibrium condition yields the expression

$$T_i^R - T_i^L + I_i \omega^2 \phi_i = 0 \quad (2.17)$$

These equations are combined in the single matrix expression

$$\begin{bmatrix} \phi \\ T \end{bmatrix}_i^R = \begin{bmatrix} 1 & 0 \\ -\omega^2 I & 1 \end{bmatrix} \cdot \begin{bmatrix} \phi \\ T \end{bmatrix}_i^L \quad (2.18)$$

or

$$z_i^R = P_i z_i^L \quad (2.19)$$

CHAPTER THREE

THEORETICAL ANALYSIS

3.1 Introduction

Before carrying out the theoretical analysis, boundary conditions, variation of cross-sections and geometric and force conditions have been specified.

The diameters of the shafts may be uniform or changing linear, parabolic (convex), parabolic (concave), along the longitudinal axis. Uniform, linear, parabolic (convex) diameters, are expressed as:

$$d(x) = d_o + zx^m \quad (3.1)$$

and

$$z = \frac{d_1 - d_o}{L^m} \quad (3.2)$$

where d_o denote the diameter of the root cross-section, d_1 are those at the tip cross-section, respectively. The diameter change uniformly where $m = 0$, linearly where $m = 1$ and parabolically where $m = 2$.

Typical shafts having different diameter variation parameters that are uniform, linear, parabolic (concav) are shown in Figures 3.1, 3.2, 3.3 .

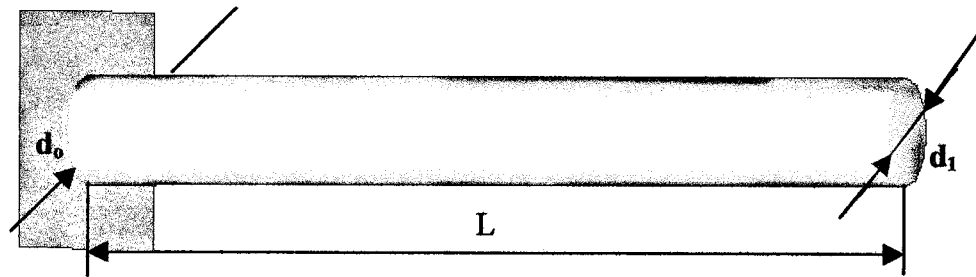


Figure 3.1 Uniform shaft

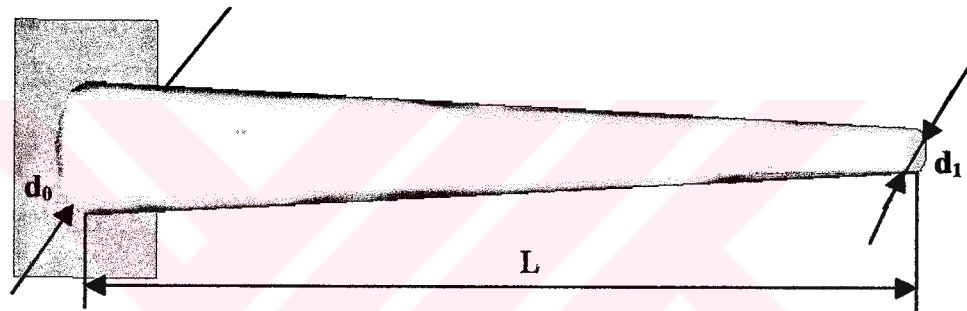


Figure 3.2 Linear (Tapered) shaft

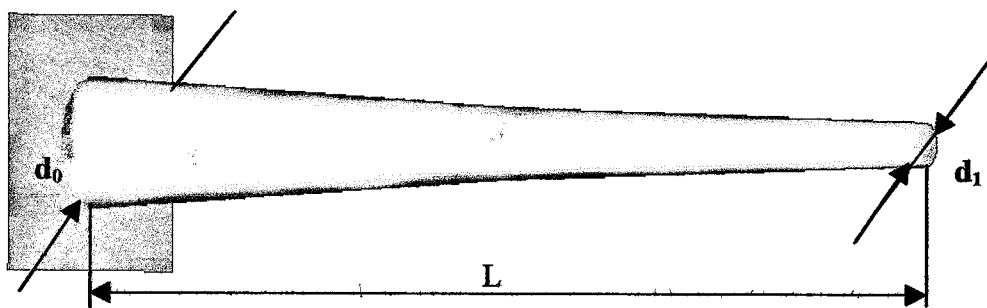


Figure 3.3 Parabolic (Concave) shaft

Variation of the diameter of a shaft having parabolic (convex) cross-sections along its length can be expressed as:

$$d(x) = \frac{2.(d_1 - d_0)x}{L} - \frac{(d_1 - d_0)x^2}{L^2} + d_0 \quad (3.3)$$

Equation (3.2) is only valid for the parabolic (convex) cross-section.

Parabolic (convex) cross-sections are shown in Figures 3.4 .

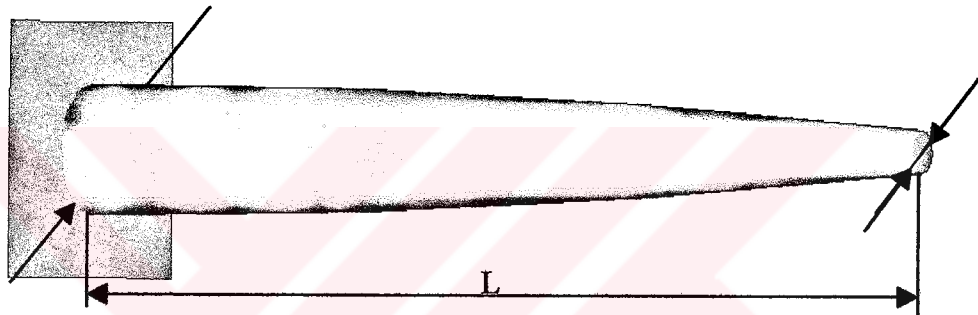


Figure 3.4 Parabolic (Convex) shaft

3.2 Determination of the Area and Second moment of Area for a Shaft Finite Element

We have four types of cross-section of the shaft. Area "A" and the second moment of area of cross-section "I" of the shaft depend on x . To simplify the analysis some assumptions made are as follows.

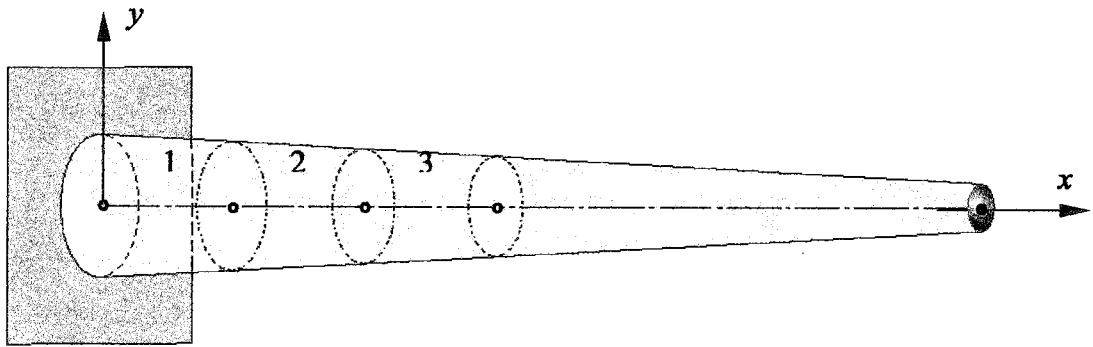


Figure 3.5 Discretizations of the shaft

The shaft is divided into finite elements. The area and second moment of area of a variable cross-sectioned shaft are different, along the shaft length and depend on x . Let us take a shaft element from Figure 3.5 into consideration.

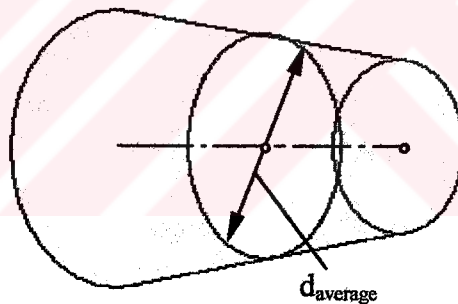


Figure 3.6 Average diameter of a shaft element

The diameter (d_x) of the element depend on x . The calculated average diameters of the shaft are denoted by d_{average} . Using this average diameter, A and I are calculated. This process is applied to each element. So we form a configuration shown in Fig. 3.7 to represent a non-uniform shaft.

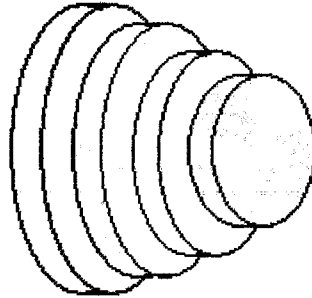


Figure 3.7 Shaft elements having average diameters

3.3 Determination of Deflections of a Finite Element

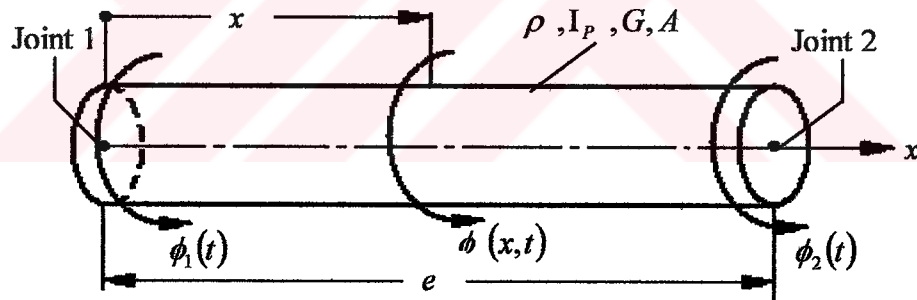


Figure 3.8 A Uniform Torsion Element

Consider a uniform torsion of element with the x axis taken along the centroidal axis, as shown in Fig. 3.8. Let I_p denotes the polar moment of inertia about the centroidal axis and GJ represent the torsional stiffness ($J=I_p$ for a circular cross section).

When the torsional displacement (rotation) within the element is assumed to be linear with respect to x , as

$$\phi(x, t) = a(t) + b(t)x \quad (3.4)$$

and the joint rotations both at ends of the element, $\phi_1(t)$ and $\phi_2(t)$ are treated as unknowns, Eq.(3.4) can be expressed, by proceeding as in the case of a bar element, as follows.

$$\phi_1(x, t) = N_1(x)\phi_1(t) + N_2(x)\phi_2(t) \quad (3.5)$$

where $N_1(x)$ and $N_2(x)$ are given as

$$N_1(x) = \left(1 - \frac{x}{e}\right), \quad N_2(x) = \frac{x}{e} \quad (3.6)$$

3.3.1 Evaluation of the Element Elastic Stiffness Matrix

The strain energy V of an elemental length on the shaft is given by

$$V(t) = \frac{1}{2} \int_0^e GJ \left\{ \frac{\partial \phi(x, t)}{\partial x} \right\}^2 dx \quad (3.7)$$

$$= \frac{1}{2} \int_0^e GJ \left\{ -\frac{1}{e}\phi_1(t) + \frac{1}{e}\phi_2(t) \right\}^2 dx \quad (3.8)$$

$$= \frac{1}{2} \cdot \frac{GJ}{e} \left\{ \phi_1^2(t) - 2\phi_1(t)\phi_2(t) + \phi_2^2(t) \right\} \quad (3.9)$$

where the element elastic stiffness matrix is described as

$$[k] = \frac{GJ}{e} \begin{bmatrix} 1 & -1 \\ -1 & 1 \end{bmatrix} \quad (3.10)$$

3.3.2 Evaluation of the Mass Matrix

The kinetic energy T of an elemental length on the shaft is given by

$$T(t) = \frac{1}{2} \int_0^e \rho I_p \left\{ \frac{\partial \phi(x,t)}{\partial t} \right\}^2 dx \quad (3.11)$$

$$= \frac{1}{2} \int_0^e \rho I_p \left\{ \left(1 - \frac{x}{e} \right) \dot{\phi}_1(t) + \frac{x}{e} \dot{\phi}_2(t) \right\}^2 dx \quad (3.12)$$

$$= \frac{1}{2} \frac{\rho I_p e}{3} \left\{ \dot{\phi}_1^2(t) + \dot{\phi}_1(t) \dot{\phi}_2(t) + \dot{\phi}_2^2(t) \right\} \quad (3.13)$$

where the mass matrix is describe as

$$[m] = \frac{\rho I_p e}{6} \begin{bmatrix} 2 & 1 \\ 1 & 2 \end{bmatrix} \quad (3.14)$$

3.4 Evaluation of the Transfer Matrix Method

The Transfer Matrix method was discussed in section 2.2. Now we will discuss how make use of the transfer matrix method in numerical calculations. We have formed stiffness and mass matrixes as discussed in section 2.2. The matrix multiplications have been made carrying ω^2 through as a free parameter, and finally applying the boundary conditions then solving the resulting frequency equation for ω^2 . This matrix operation,

which relates the state vectors z_{i-1}^R and z_i^R , is illustrated here for a disk-shaft system (Fig 3.9)

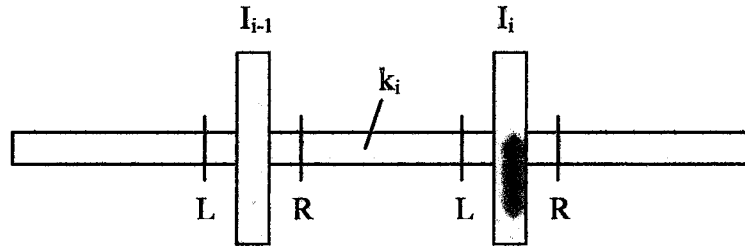


Figure 3.9 Shaft-Disk System

The relation between z_{i-1}^R and z_i^L is given by

$$\begin{bmatrix} \phi \\ T \end{bmatrix}_i^L = \begin{bmatrix} 1 & 1/k \\ 0 & 1 \end{bmatrix}_i \cdot \begin{bmatrix} \phi \\ T \end{bmatrix}_{i-1}^R \quad (3.15)$$

and that between z_{i-1}^L and z_i^R is

$$\begin{bmatrix} \phi \\ T \end{bmatrix}_i^R = \begin{bmatrix} 1 & 0 \\ -I\omega^2 & 1 \end{bmatrix}_i \cdot \begin{bmatrix} \phi \\ T \end{bmatrix}_i^L \quad (3.16)$$

Employing the standard layout for matrix multiplication gives the following expression

$$\begin{aligned} & \begin{bmatrix} 1 & 1/k \\ 0 & 1 \end{bmatrix}_i \cdot \begin{bmatrix} \phi \\ T \end{bmatrix}_{i-1}^R = \begin{bmatrix} \phi \\ T \end{bmatrix}_i^L \\ & \begin{bmatrix} 1 & 0 \\ -I\omega^2 & 1 \end{bmatrix}_i \cdot \begin{bmatrix} 1 & 1/k \\ -I\omega^2 & 1 - I\omega^2/k \end{bmatrix}_i \cdot \begin{bmatrix} \phi \\ T \end{bmatrix}_{i-1}^R = \begin{bmatrix} \phi \\ T \end{bmatrix}_i^R \end{aligned} \quad (3.18)$$

Hence

$$\phi_i^L = \phi_i^R = \phi_{i-1}^R + \frac{T_{i-1}^R}{k_i} \quad (3.19)$$

and

$$T_i^R = -\omega^2 I_i x_{i-1}^R + \left(1 - \frac{\omega^2 I_i}{k_i}\right) T_{i-1}^R \quad (3.20)$$

$$= T_{i-1}^R - \omega^2 I_i \left(x_{i-1}^R + \frac{T_{i-1}^R}{k_i} \right) = T_{i-1}^R - \omega^2 I_i x_i^L \quad (3.21)$$

The same result are obtained by using the following layout, which combines the field and the point matrix into a single matrix:

$$\begin{bmatrix} \phi \\ T \end{bmatrix}_{i-1}^R \cdot \begin{bmatrix} 1 & 1/k & 0 \\ 0 & 1 & -\omega^2 I \end{bmatrix}_i \cdot \begin{bmatrix} a \\ b \end{bmatrix} = \begin{bmatrix} \phi \\ T \end{bmatrix}_i^R = z_i^R \quad (3.22)$$

The element $a \equiv \phi_i^R = \phi_i^L$ is found in the usual way:

$$\begin{bmatrix} \phi \\ T \end{bmatrix}_{i-1}^R \cdot \begin{bmatrix} 1 & 1/k \end{bmatrix} \cdot [a] = (1)\phi_{i-1}^R + \frac{T_{i-1}^R}{k_i} = \phi_i^L = \phi_i^R \quad (3.23)$$

and the element b is computed as if the element a belonged to the column vector z_{i-1}^R :

$$\begin{bmatrix} \phi_{i-1}^R \\ T_{i-1}^R \\ a \end{bmatrix}$$

$$\begin{bmatrix} 0 & 1 & -\omega^2 I_i \end{bmatrix} \cdot [b] = (0)x_{i-1}^R + T_{i-1}^R - \omega^2 I_i a \quad (3.24)$$

Since $a = \phi_i^R$, we have indeed

$$b = T_{i-1}^R - \omega^2 I_i \phi_i^R = T_i^R \quad (3.25)$$

so that by this matrix operation we have done the equivalent to forming the product

$$z_i^R = P_i F_i z_{i-1}^R. \quad (3.26)$$

CHAPTER FOUR

RESULTS AND DISCUSSION

The vibration analysis of the system in Fig. 4.1 has been carried out, the lengths and diameters of the first, second and third segments of the shaft are changed in such a way that the stiffness of the segments were kept constant, by using the Finite Element and the Matrix Methods. The results obtained using those different methods and given in Reference [1] are compared in Table 4.1 and good agreement is found. Since the dimensions are not different for the three cases and the stiffness is constant, frequencies do not seem take as different as expected.

The variation of the first natural frequency of the system, shown in Fig 4.2, with respect to torsional stiffness is shown in graphical form in Fig. 4.3. As seen from the figure if the torsional stiffness increases, the first natural frequency also increases. The comparison of the results obtained by using the Finite Element and the Transfer Matrix Methods shows a very good agreement.

Fig. 4.4 shows the effect of the inertia of the discs on the first natural frequency for the system shown in Fig. 4.2. As seen from this figure, if the inertias of the discs increase, the first natural frequency decreases. The comparison of the results obtained using those two different methods gives very good agreement.

Fig. 4.5 shows the variation of the first natural frequency with respect to shaft stiffness as well as the number of discs having the same mass moment of inertia ($I=3.389376 \text{ kg.m}^2$) located on the shaft at equal distances from each other. As seen

from this figure, if the torsional stiffness increases, the first natural frequency also increases and if the number of the discs increases, the first natural frequency decreases.

Fig. 4.6 shows the variation of the first natural frequency with respect to disc inertia as well as the number of discs having the same mass moment of inertia while all the stiffnesses of the segments of the shaft ($k=112979.2$ Nm/rad) are kept constant. As seen from this figure, if the inertia of the discs increases, the first natural frequency decreases and if the number of the discs increases, the first natural frequency decreases.

The variations of the first and second natural frequencies of the system, shown in Fig. 4.7, with respect to the distance of the middle disc from the first disc as well as the inertia of the discs are shown in graphical forms in Fig. 4.8 and 4.9. As seen from Fig. 4.8, if the distance of the middle disc from the first disc increases until the middle of the shaft, the first natural frequency also increases and when the disc passes the middle of the shaft, the first natural frequency decreases. As seen from Fig. 4.9, if the distance of the middle disc from the first disc increases until the middle of the shaft, the second natural frequency also decreases and when the disc passes the middle of the shaft, the first natural frequency increases. As seen from these figures the results obtained are symmetric with reference to the midpoint of the shaft. The figures also show that when the mass moment of inertia increases, frequencies decrease as expected.

The variation of the first and second natural frequencies of the system, shown in Fig. 4.10, with respect to the distance of the first disc from the clamped support as well as the inertia of the discs are shown in graphical forms in Fig. 4.11 and 4.12. As seen from Fig. 4.11, if the distance of the first disc from the clamped support increases, the first natural frequency decreases.

The variations of the first and second natural frequencies of the system shown, in Fig. 4.13, with respect to the distance of the first disc from the left clamped support as well as the inertia of the discs are shown in graphical forms in Fig. 4.14 and 4.15. As seen

from Fig. 4.14, if the distance of the disc from the left clamped support increases until the middle of the shaft, the first natural frequency decreases and when the disc passes the middle of the shaft, the first natural frequency increases. As seen from Fig. 4.15, if the distance of the disc from the left clamped support increases until the middle of the shaft, the second natural frequency increases and when the disc passes the middle of the shaft, it decreases. As seen from these figures the results obtained are symmetric with reference to the mid-point of the shaft.

The variation of the first and second natural frequencies of the system, shown in Fig. 4.16, with respect to the distance of the middle two discs from the left and right discs as well as the inertia of the discs are shown in graphical forms in Fig. 4.17 and 4.18. As seen from Fig. 4.17, if the distances of the middle two discs from the left and right discs increase, the first natural frequency also increases. As seen from Fig. 4.18, if the distances of the middle two discs from the left and right discs increase, the second natural frequency decreases.

The variations of the first and second natural frequencies of the system, shown in Fig. 4.19 with respect to the distance of the middle two discs from the left clamped support and the right disc as well as the inertia of the discs are shown in graphical forms in Fig. 4.20 and 4.21. As seen from Fig. 4.20, if the distance of the middle two discs from the left clamped support and the right disc increases, the first natural frequency also increases. As seen from Fig. 4.21, if the distance of the middle two discs from the left clamped support and the right disc increases, the second natural frequency also decreases.

The variations of the first and second natural frequencies of the system, shown in Fig. 4.22, with respect to the distance of the middle two discs from the left and the right clamped supports as well as the inertia of the discs are shown in graphical forms in Fig. 4.23 and 4.24. As seen from Fig. 4.23, if the distances of the middle two discs from the left and the right clamped supports increase, the first natural frequency also decreases.

The variations of the first natural frequency of the systems, shown in Figs. 4.25, 4.27 and 4.29, with respect to initial diameter increase of the tapered shafts as well as the inertia of the discs are shown in graphical forms in Fig. 4.26, 4.28 and 4.30. As seen from these figures that, if the first diameter of the tapered shaft increases the first natural frequency also increases and if the inertia of the discs increases the first natural frequency decreases.

Table 4.2 gives the comparison of the first natural frequency results of the systems shown in Fig. 4.27 and 4.29. As seen from this table if the inertia of disc increases, the differences between the results of the natural frequency of the two systems decreases because inertia of the discs dominates the vibration of the system. The system with right hand side support is stiffer than the other as a result the frequencies are higher.

The variations of the first natural frequency of the systems, shown in Fig 4.30, with respect to the first diameter of the tapered, concave and convex shafts are shown in graphical forms in Fig 4.32. As seen from this figure if the initial diameter of the shafts increases, the first natural frequency also increases.

The variation of the first natural frequency of the systems, shown in Fig 4.30, with respect to the length of the tapered, concave and convex shafts are shown in graphical forms in Fig 4.33. As seen from this figure if the length of the shafts increases, the first natural frequency also decreases.

The variation of the first natural frequency of the systems, shown in Fig 4.30, with respect to the mass moment of inertia of the discs is shown in graphical form in Fig 4.34. As seen from this figure that if the inertia of the discs increases, the first natural frequency decreases.

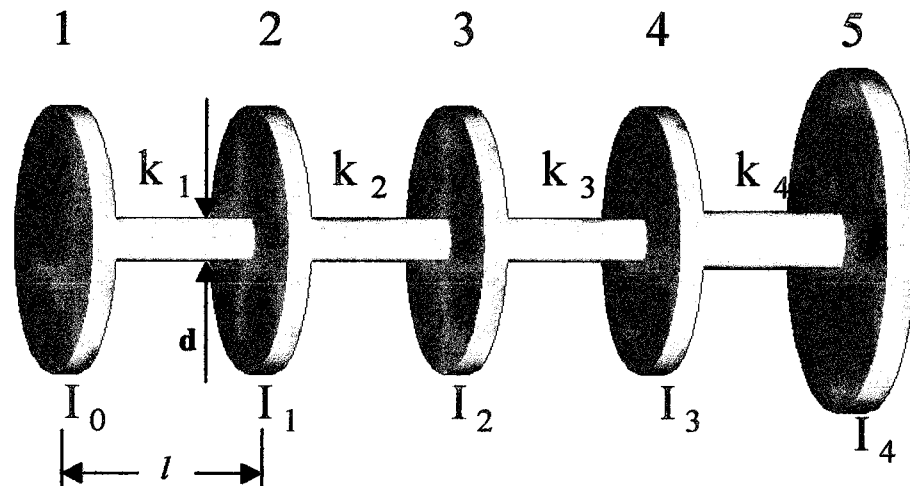


Figure 4.1 Idealized machine shaft.

The idealized representation of a four cylinder engine with a flywheel attached is shown in Fig.4.1.

$$I_0 = I_1 = I_2 = I_3 = 1.129792 \text{ kg.m}^2 \quad (10 \text{ lb-in.-sec}^2)$$

$$I_4 = 2.259584 \text{ kg.m}^2 \quad (20 \text{ lb-in.-sec}^2)$$

$$k_1 = k_2 = k_3 = 169468.8 \text{ Nm/radian} \quad (1.5 \times 10^6 \text{ lb-in./radian})$$

$$k_4 = 225958.4 \text{ Nm/radian} \quad (2.0 \times 10^6 \text{ lb-in./radian})$$

In this system we change once, twice and third shaft's length and diameter and solve with Finite Element Method. On the other hand this system solve with Transfer Matrix Method.

Table 4.1 Comparison with Finite Element Method and Transfer Matrix Method.

| | Finite Element | | | Transfer Matrix | Reference [1] |
|------------|--|---------------------------|----------------------------|-----------------|---------------|
| | $l = 1$ $d = 0.0675$ | $l = 0.5$ $d = 0.0567$ | $l = 0.25$ $d = 0.0477$ | | |
| | $k = 169468.8 \left(\frac{Nm}{rad} \right)$ | | | | |
| ω_2 | 213.672 | 214.193 | 214.283 | 214.358 | 214.337 |
| ω_3 | 443.01 | 442.709 | 444.5 | 444.673 | ≈ 440 |
| ω_4 | 632.262 | 633.771 | 634.024 | 634.245 | ≈ 625 |
| ω_5 | 742.452 | 743.899 | 744.114 | 744.345 | ≈ 750 |

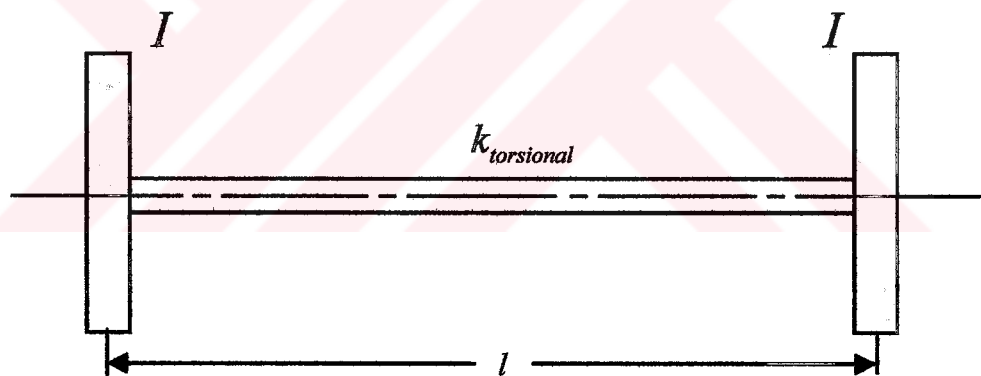


Figure 4.2 Two disks-shaft system with, free-free support condition. $I=3.389 \text{ kg.m}^2$ $l=0.5 \text{ m}$

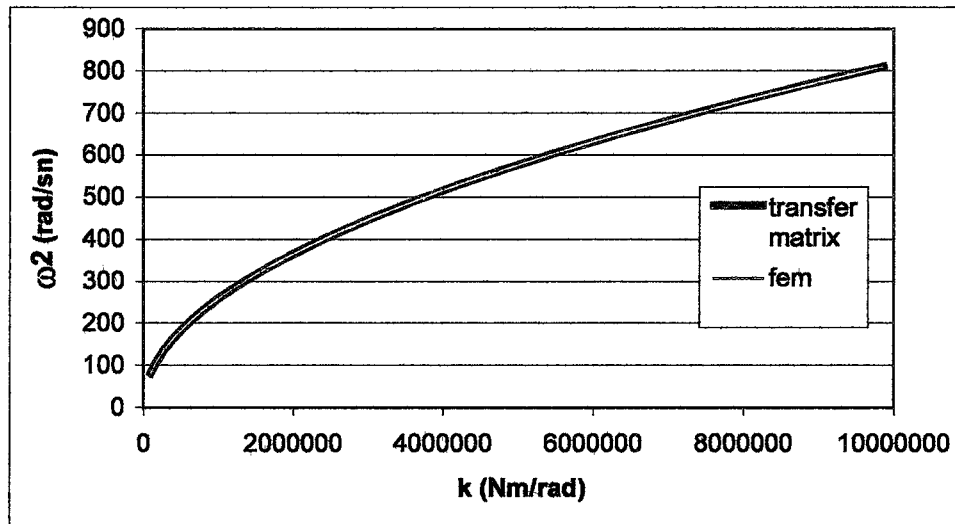


Figure 4.3 Comparison of the results of the Finite Element and the Transfer Matrix Methods with respect to torsional stiffness on the natural frequency of vibration for a multi disc-shaft system (Fig. 4.2). $n=2$, $I=3.389 \text{ kg.m}^2$, $l=0.5 \text{ m}$

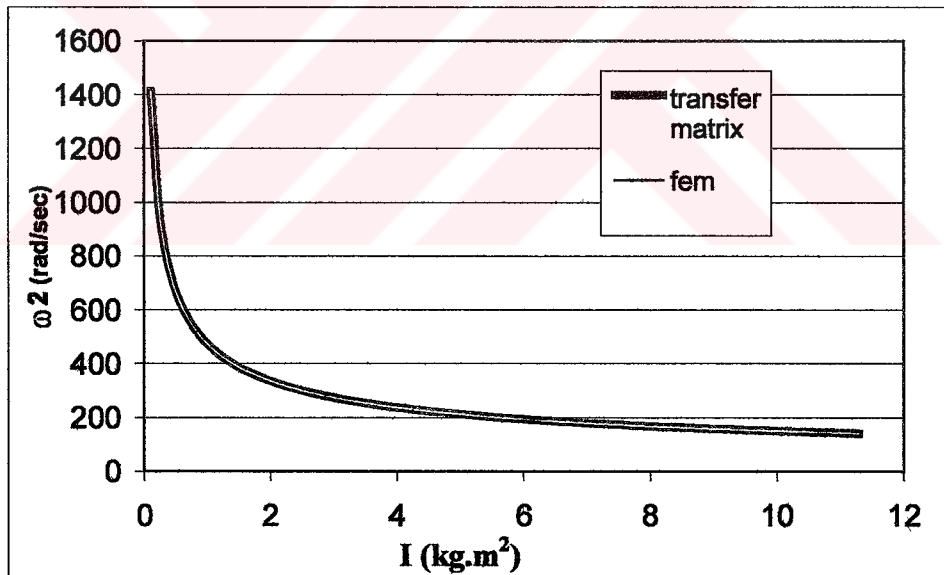


Figure 4.4 Comparison of the results of the Finite Element and the Transfer Matrix Methods with respect to disc inertia on the natural frequency of vibration for a multi disc-shaft system (Fig. 4.2) $n=2$, $I=3.389 \text{ kg.m}^2$, $l=0.5 \text{ m}$

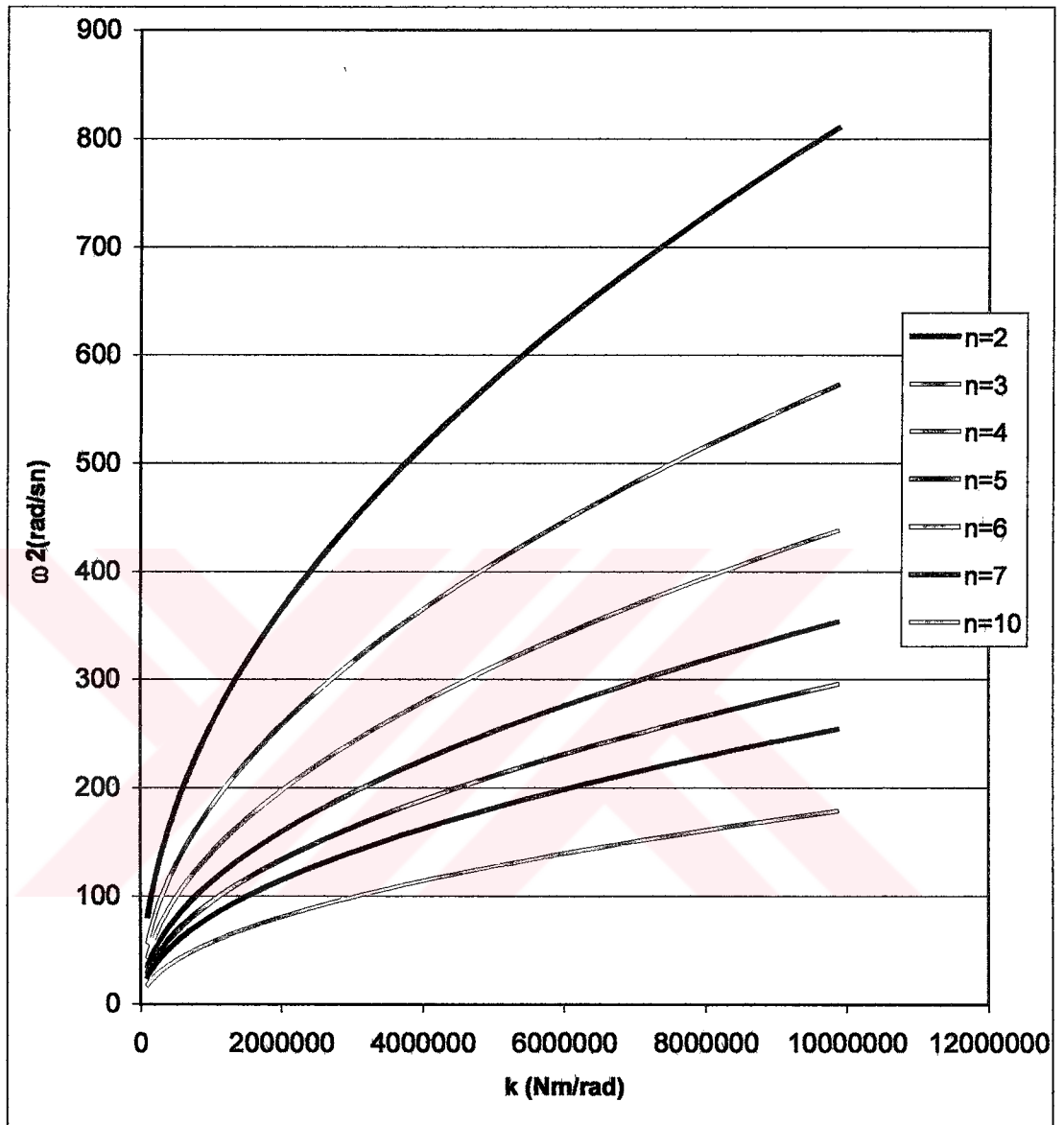


Figure 4.5 The effects of torsional stiffness and the number of discs on the first natural frequency of vibration.

$$I=3.38937 \text{ kg.m}^2$$

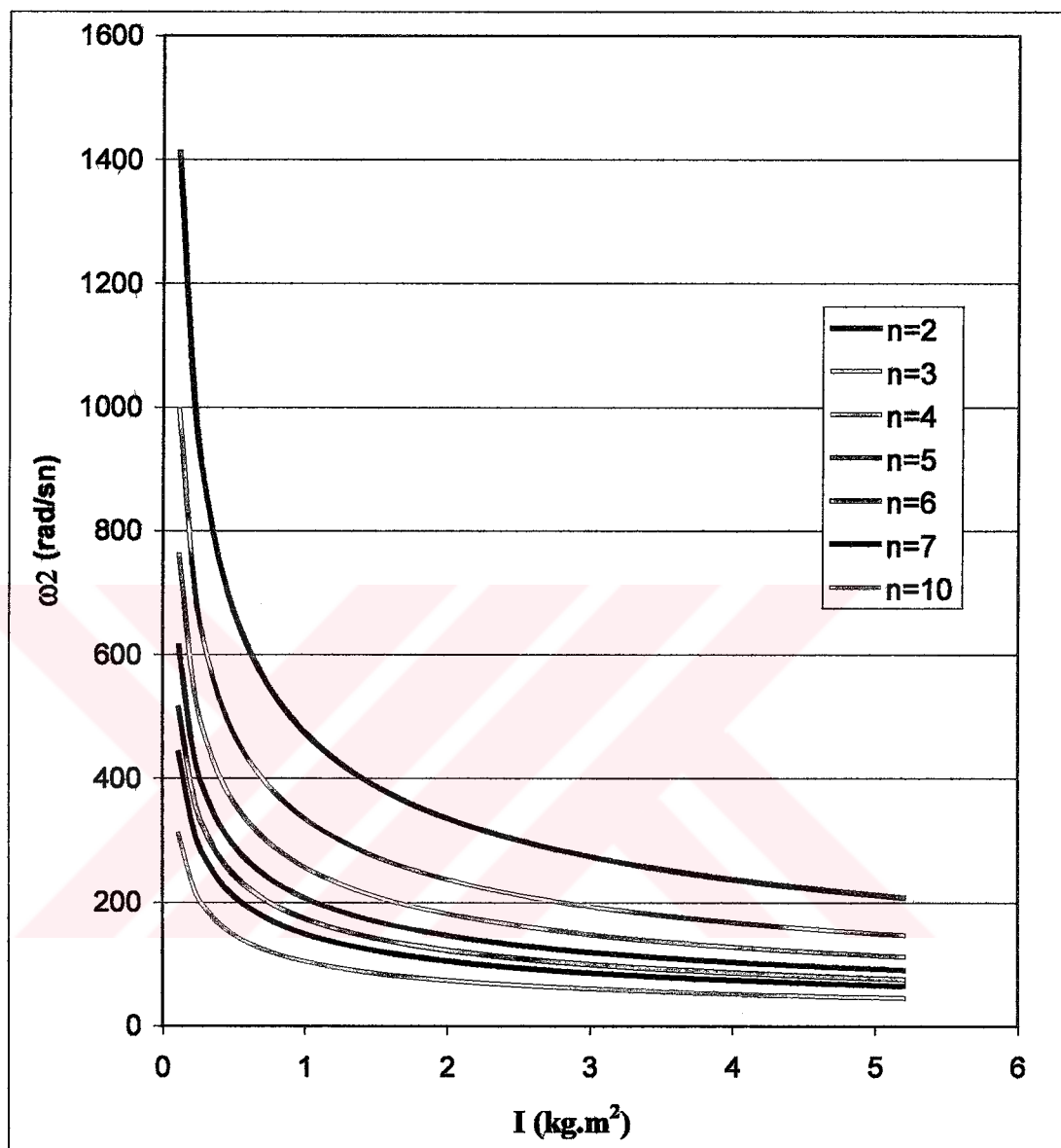


Figure 4.6 The effects of torsional stiffness and the number of discs on the first natural frequency of vibration
 $k=112979.2 \text{ Nm/rad}$

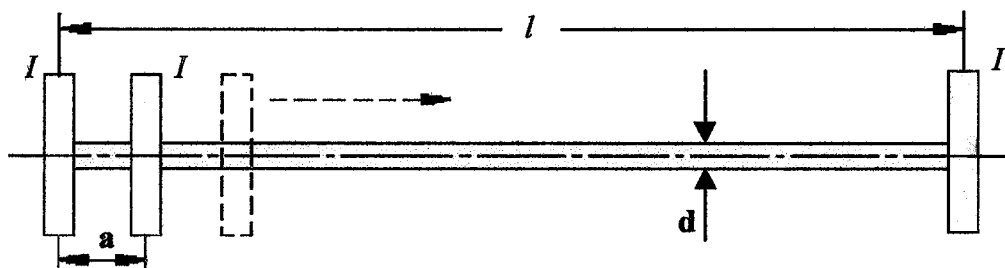


Figure 4.7 The multi disk-shaft system that having disk with free-free support condition. $l=1$ m, $d=0.05$ m

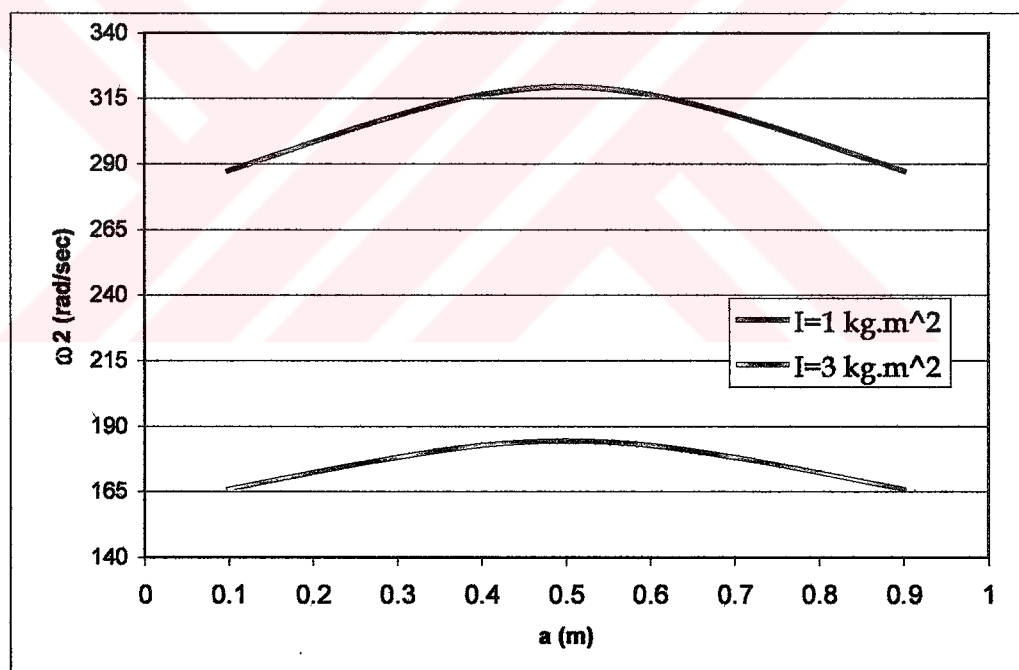


Figure 4.8 The effects of the distance of the middle disk from the first disk and the disks inertias on the second natural frequency of vibration.

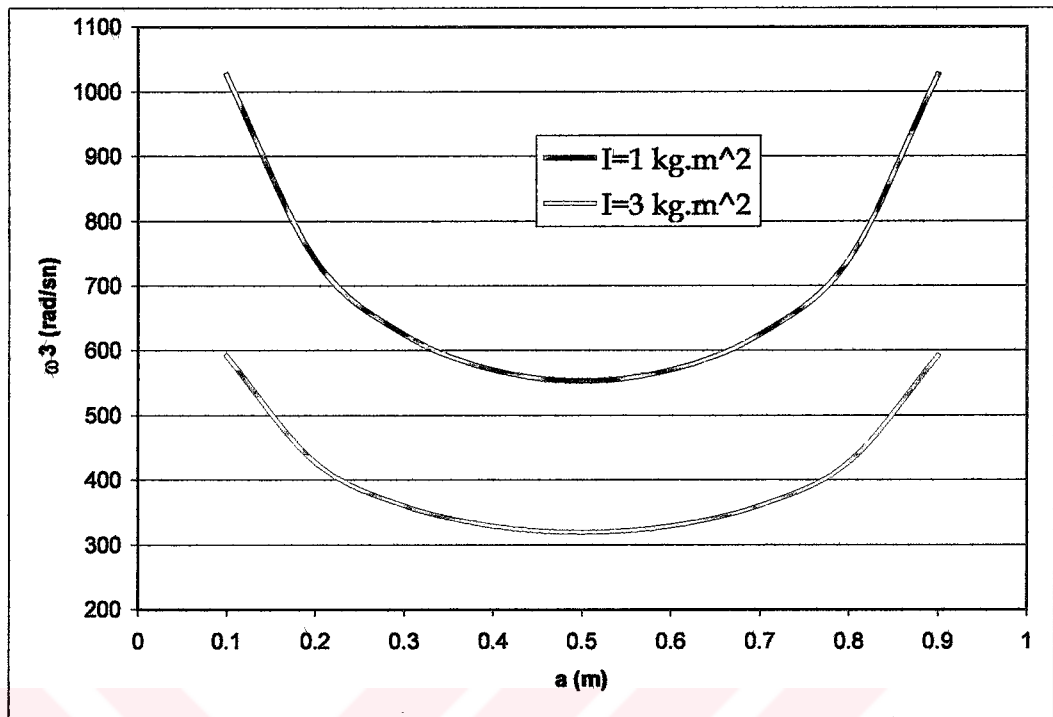


Figure 4.9 The effects of the distance of the middle disk from the first disk and the disks inertias on the third natural frequency of vibration.

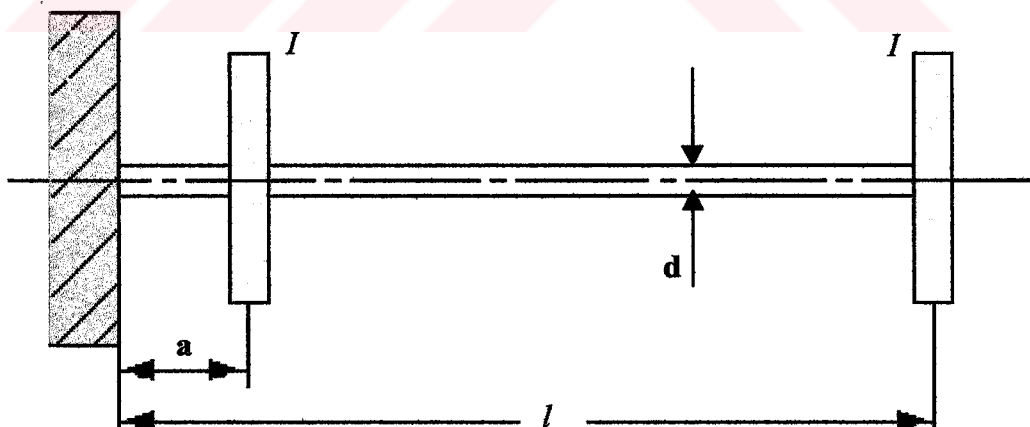


Figure 4.10 The multi disk-shaft system having two disk with clamped- free support condition. $l=1$ m, $d=0.05$ m

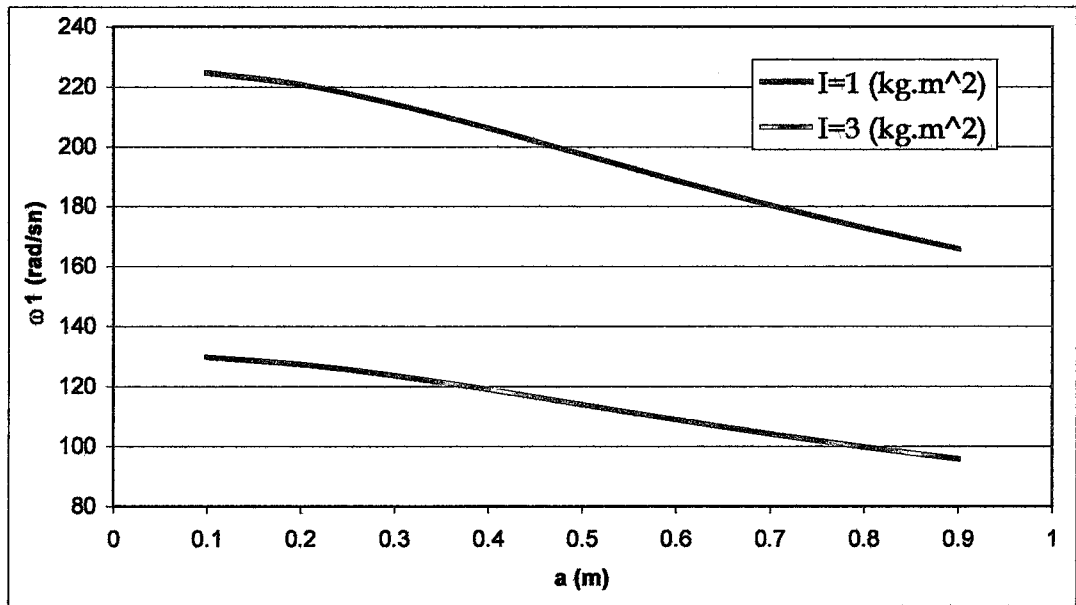


Figure 4.11 The effects of the distance of the middle disk from the clamped support and the disks inertias on the first natural frequency of vibration.

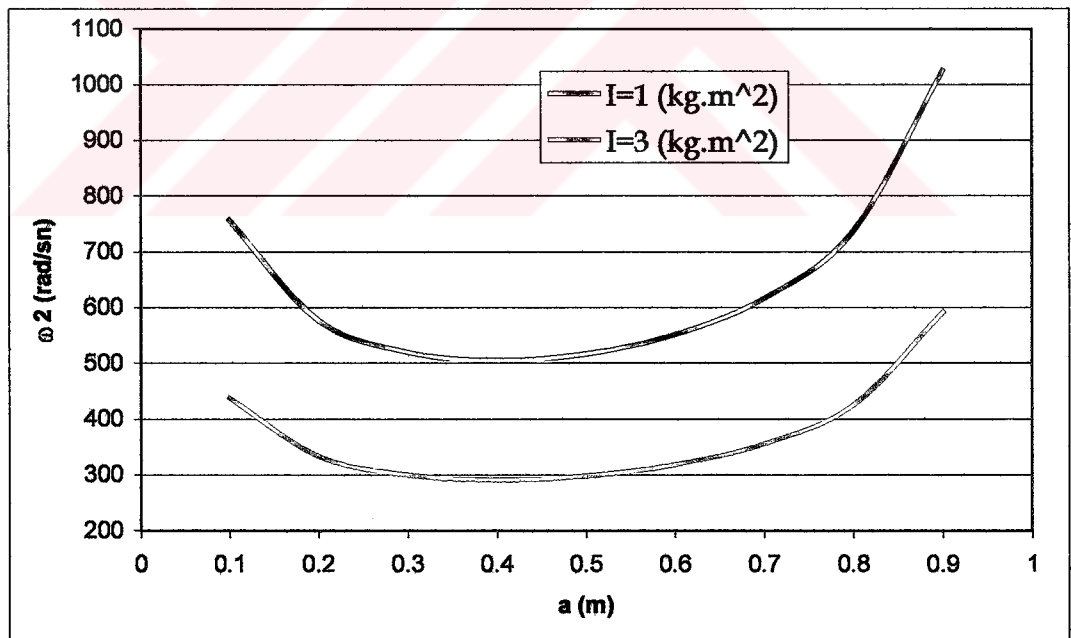


Figure 4.12 The effects of the distance of the middle disk from the clamped support and the disks inertias on the second natural frequency.

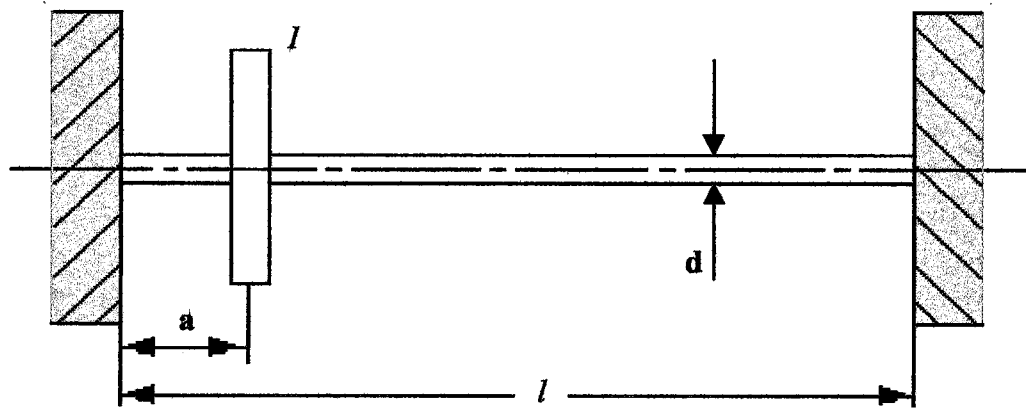


Figure 4.13 The single disk-shaft system with clamped-clamped support condition. $l=1$ m, $d=0.05$ m

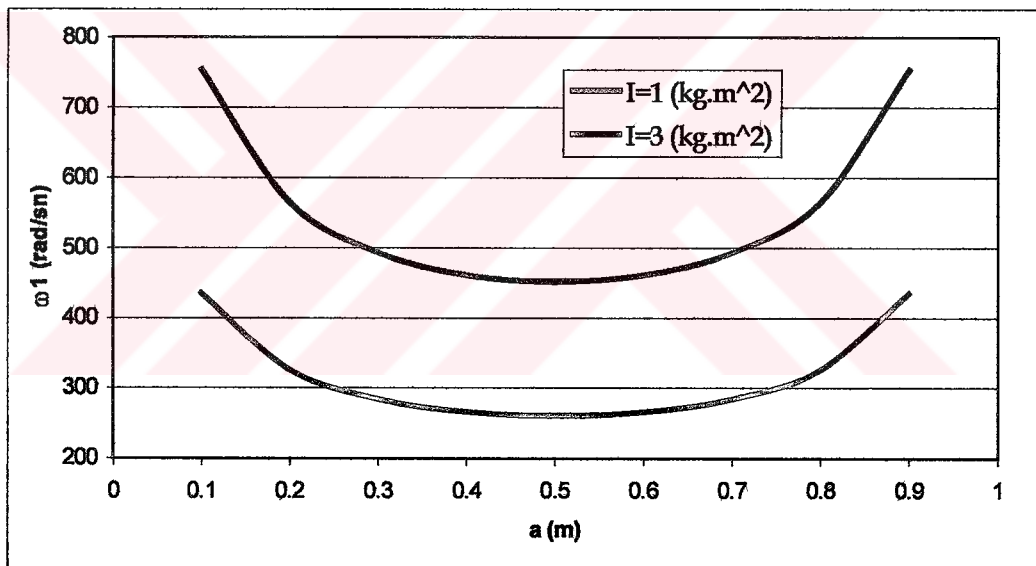


Figure 4.14 The effects of the distance of the disk from the left clamped support and the disk inertia on the first natural frequency.

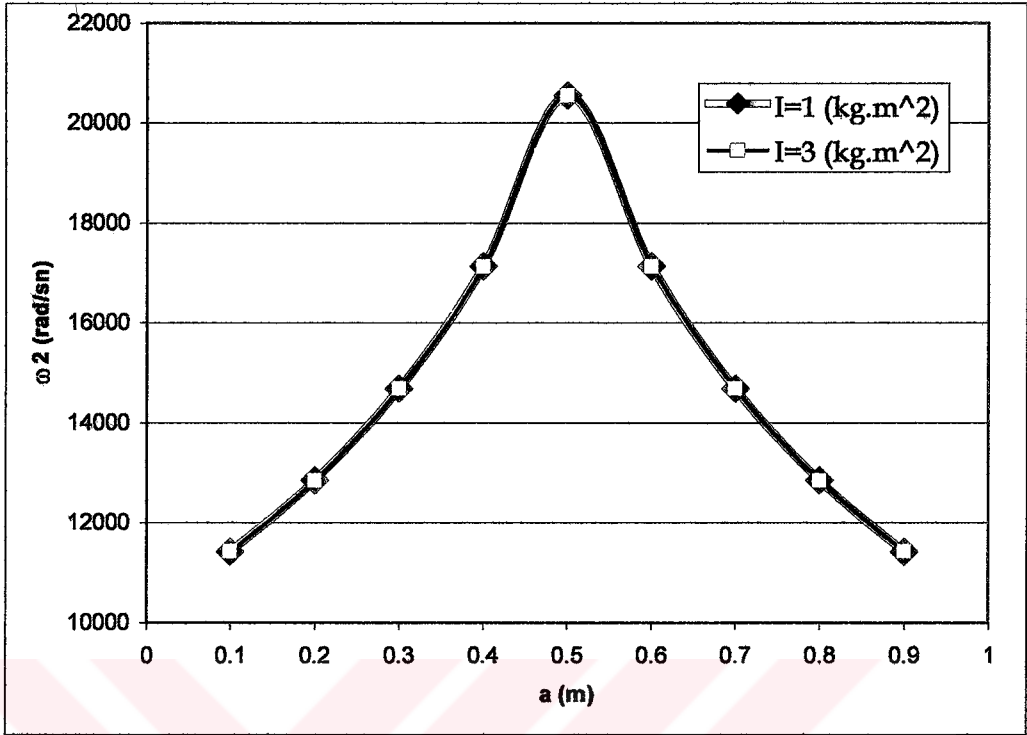


Figure 4.15 The effects of the distance of the disk from the left clamped support and the disk inertia on the second natural frequency.

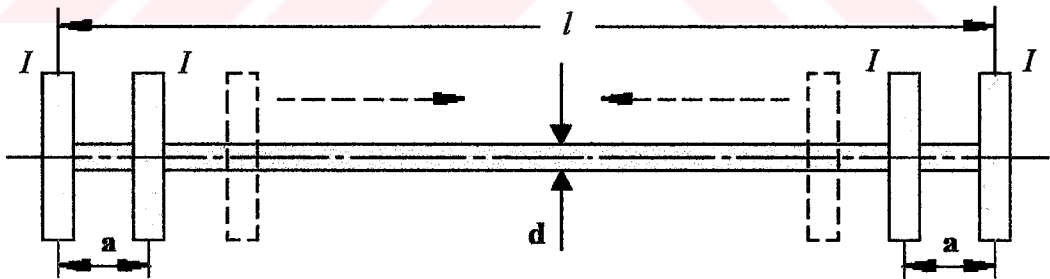


Figure 4.16 The multi disk-shaft system having four disk with free-free support condition. $l=1$ m, $d=0.05$ m

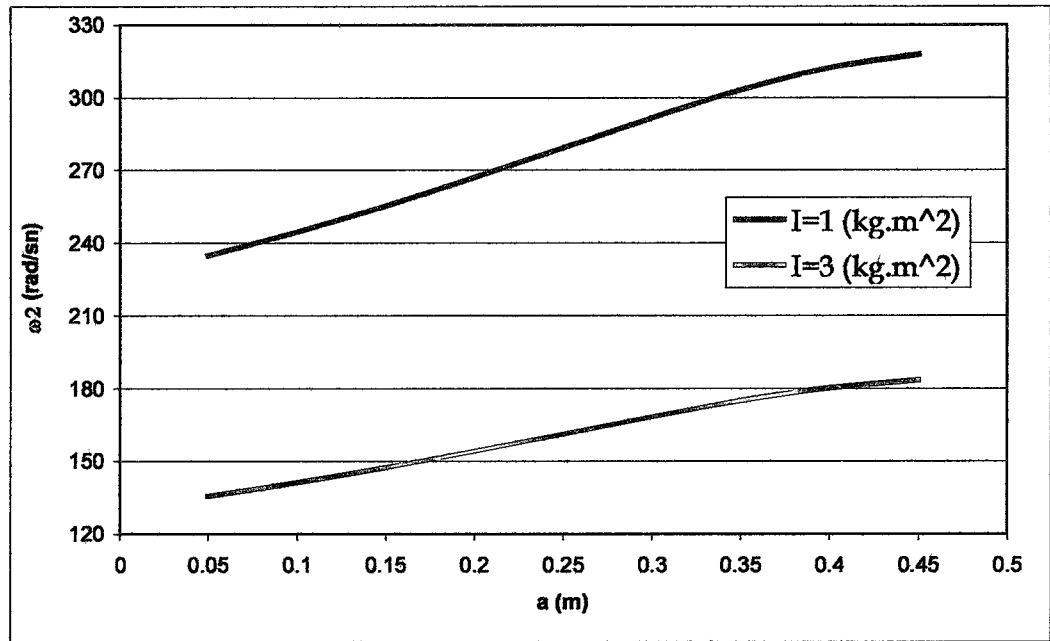


Figure 4.17 The effects of the distance of the middle two disk from the left and right discs and the disks inertias on the second natural frequency.

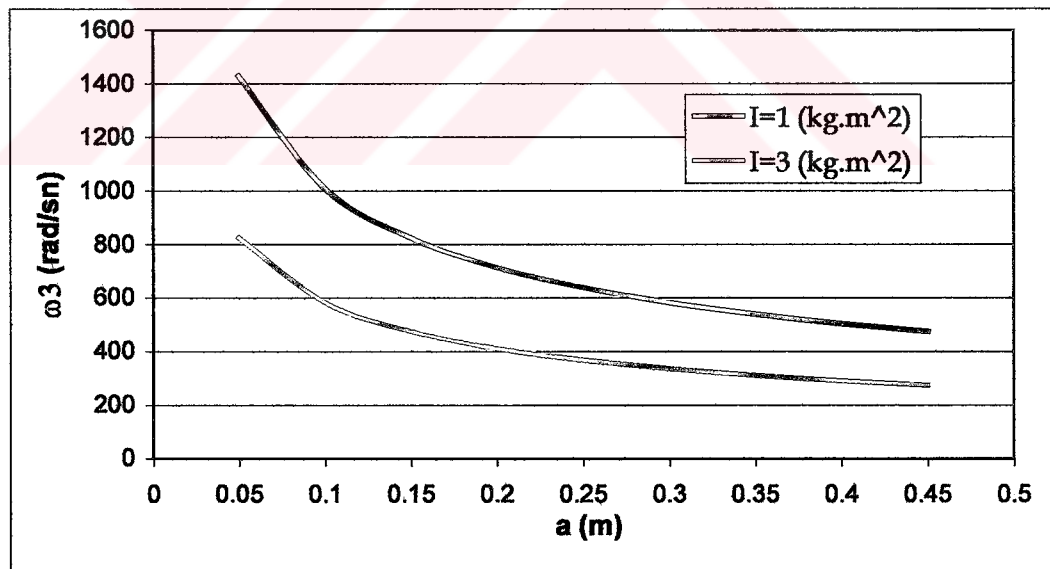


Figure 4.18 The effects of the distance of the middle two disk from the left and right discs and the disks inertias on the third natural frequency.

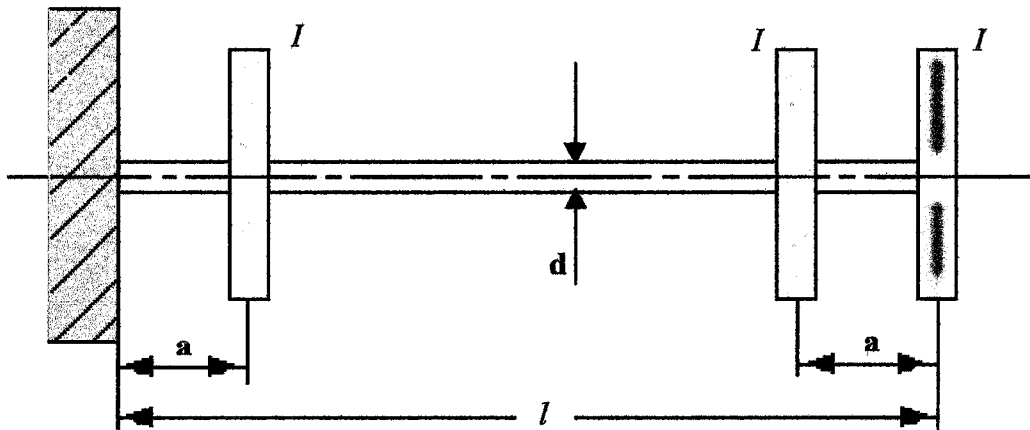


Figure 4.19 The multi disk-shaft system having three disk with clamped-free support condition. $l=1$ m, $d=0.05$ m

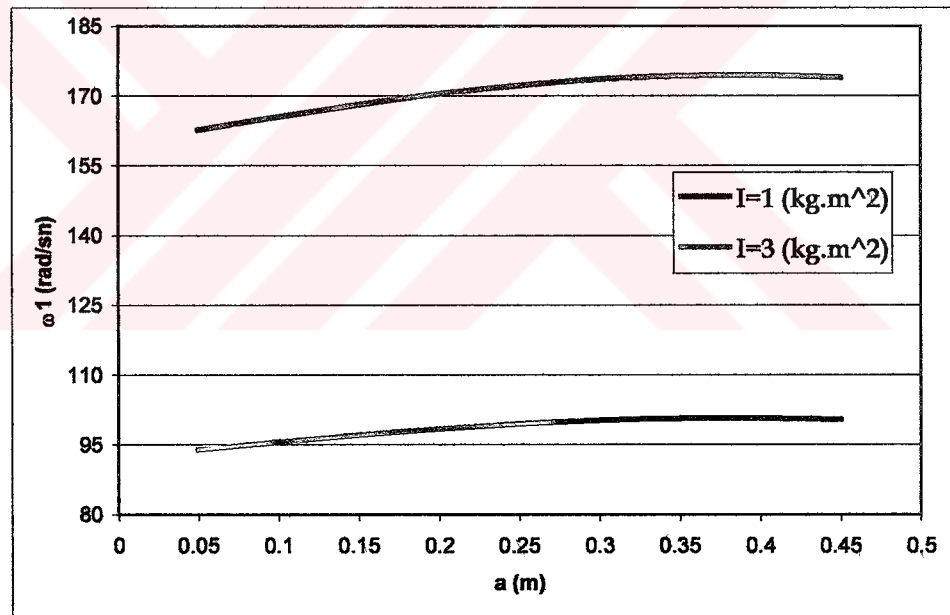


Figure 4.20 The effects of the distance of the middle two disc from the left clamped support and the right disc and the discs inertias on the first natural frequency of vibration.

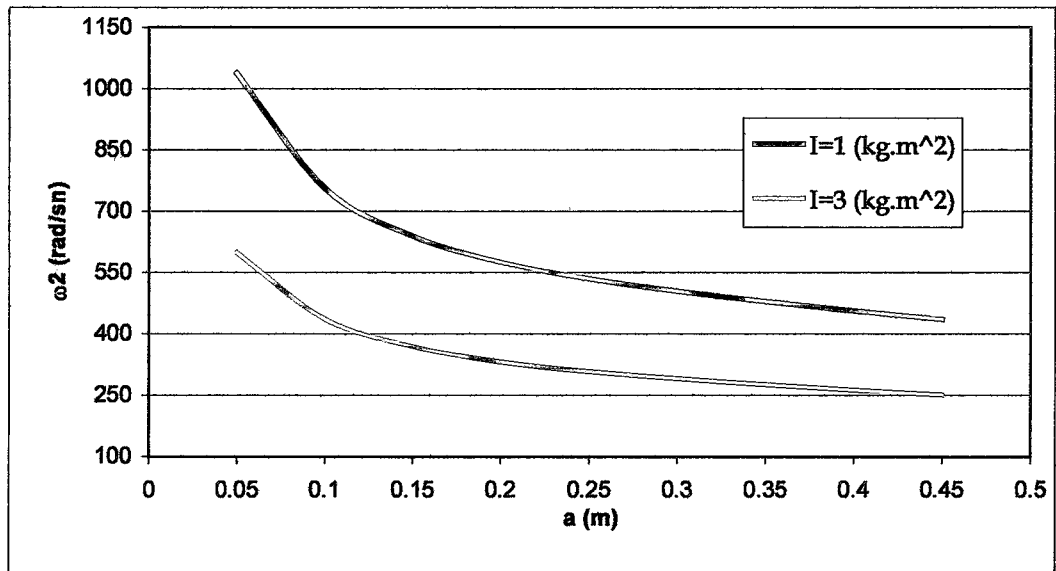


Figure 4.21 The effects of the distance of the middle two disc from the left clamped support and the right disc and the discs inertias on the second natural frequency of vibration.

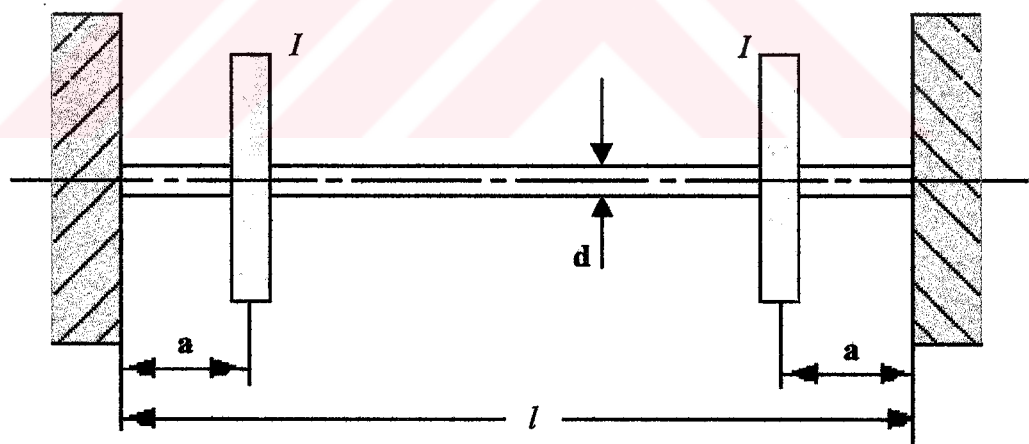


Figure 4.22 The multi disk-shaft system having two disk with clamped-clamped support condition $l=1$ m, $d=0.05$ m

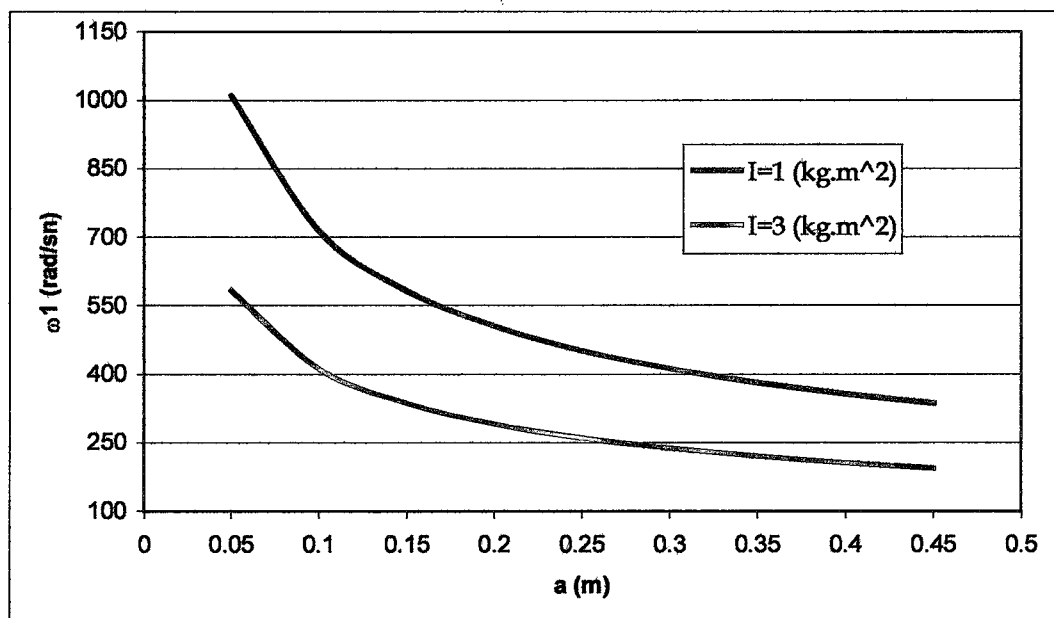


Figure 4.23 The effects of the distance of the middle two disk from the left and right clamped support and the discs inertias on the first natural frequency of vibration.

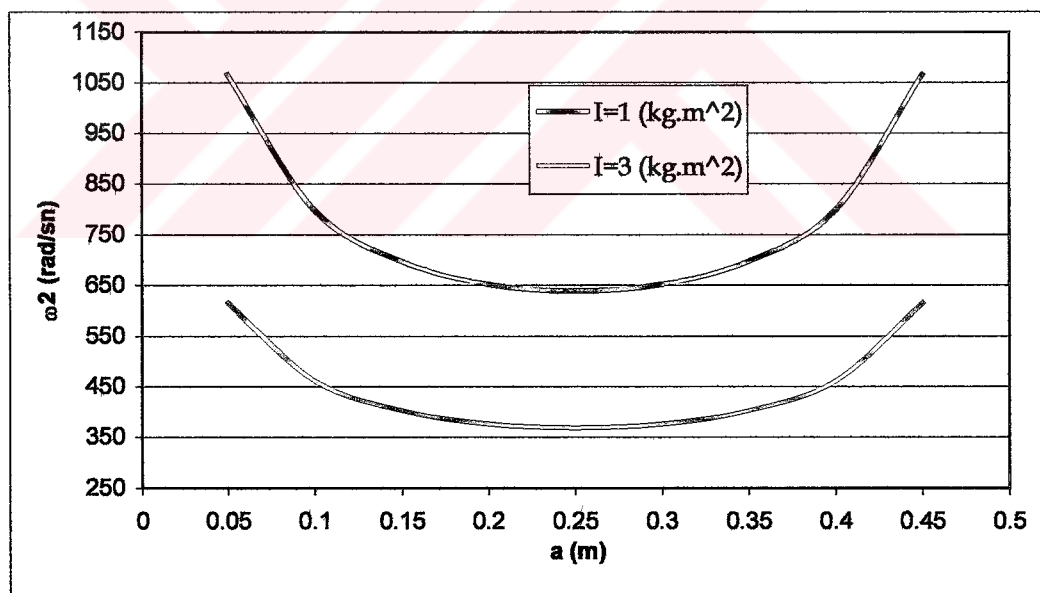


Figure 4.24 The effects of the distance of the middle two disk from the left and right clamped support and the discs inertias on the second natural frequency of vibration.

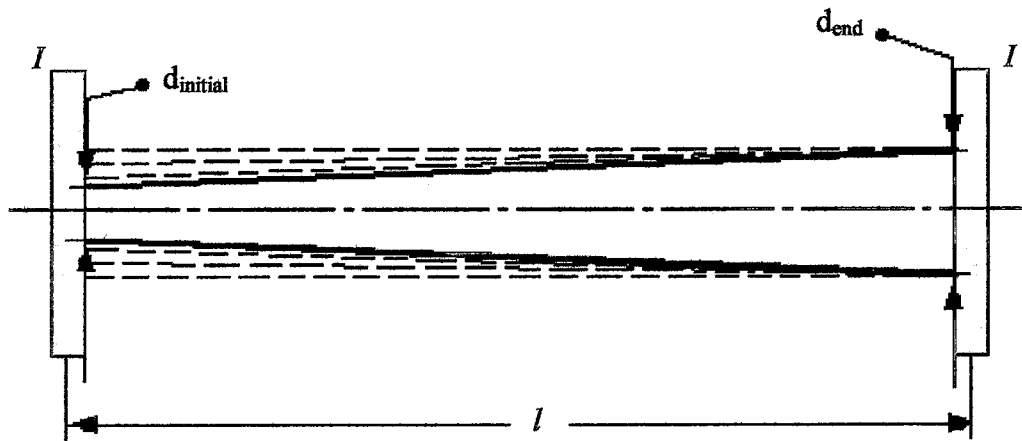


Figure 4.25 The multi disc-shaft system having two disk and tapered shaft with free-free support condition.

$$l=1 \text{ m} \quad d_{\text{initial}}=0.05 \text{ m} \quad d_{\text{end}}=0.15 \text{ m}$$

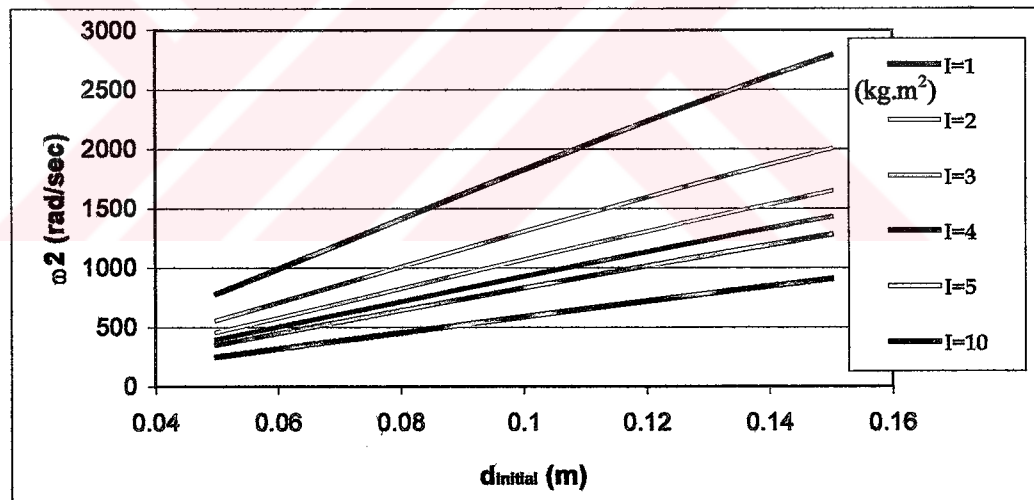


Figure 4.26 The effects of changing initial diameter and the inertia of the disks on the second natural frequency of vibration for the system shown in Fig. 4.25.

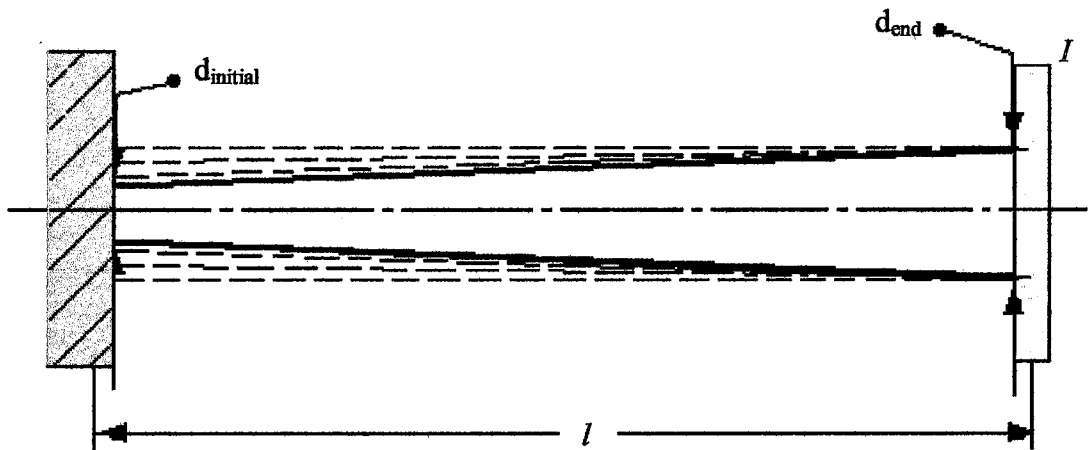


Figure 4.27 The disc-shaft system having a disk and tapered shaft with clamped-free support condition.

$$l=1 \text{ m} \quad d_{\text{initial}}=0.05 \text{ m} \quad d_{\text{end}}=0.15 \text{ m}$$

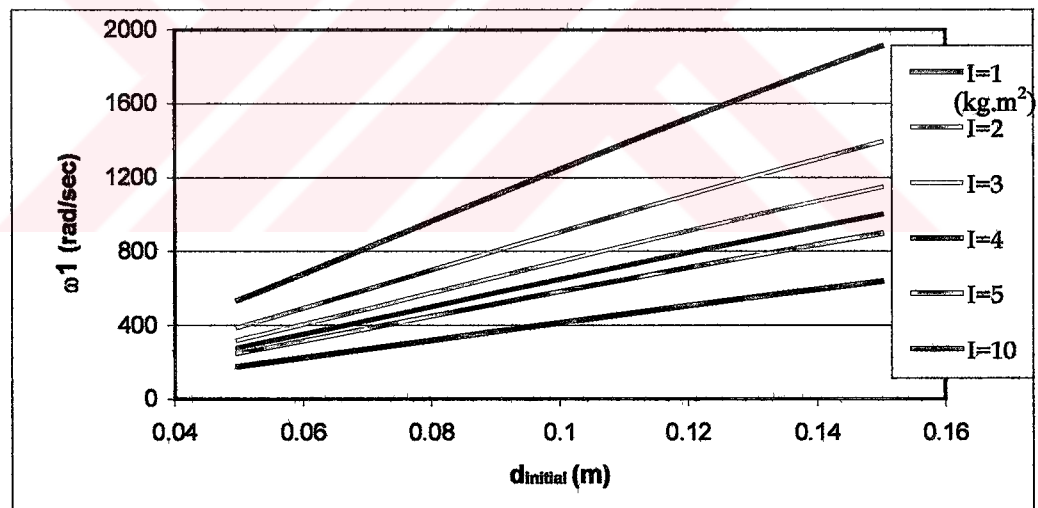


Figure 4.28 The effects of changing initial diameter of tapered shaft and the inertia of the disk on the first natural frequency of vibration for the system shown in Fig. 4.27

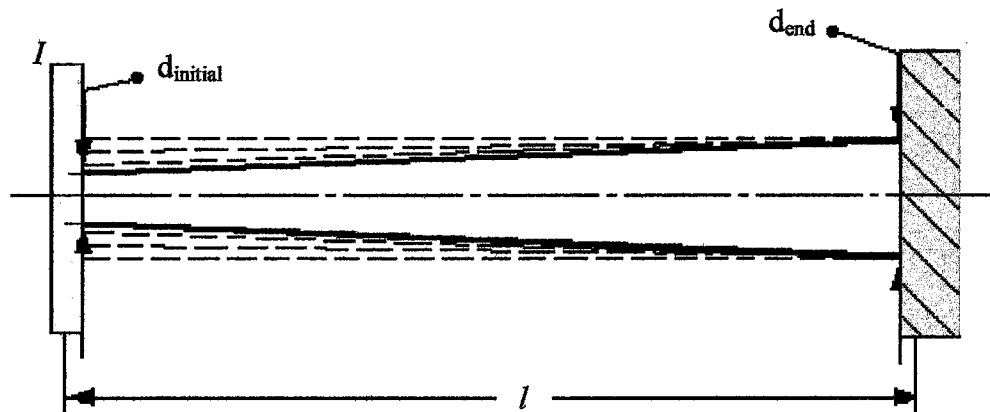


Figure 4.29 The disc-shaft system having a disk and tapered shaft with free-clamped support condition.

$$l=1 \text{ m} \quad d_{\text{initial}}=0.05 \text{ m} \quad d_{\text{end}}=0.15 \text{ m}$$

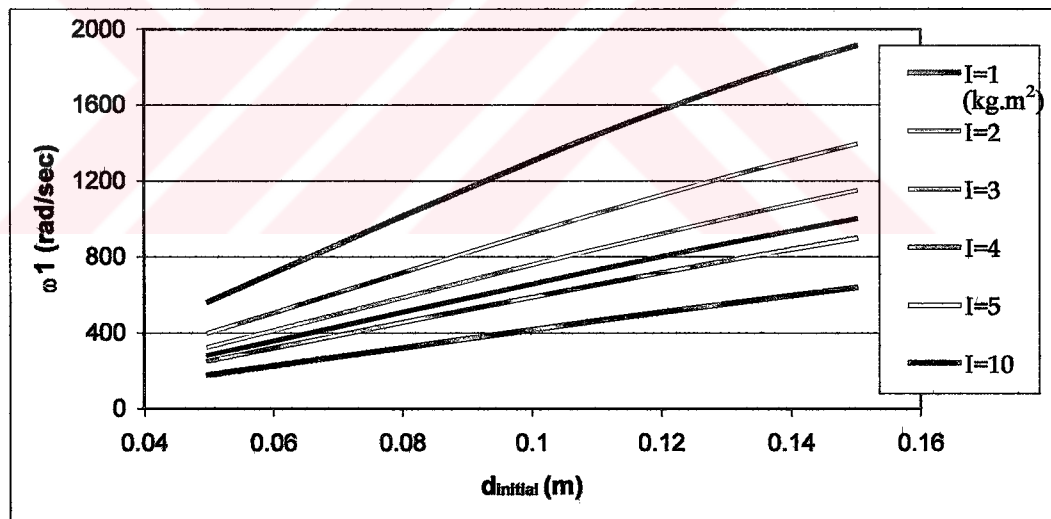


Figure 4.30 The effects of changing initial diameter of tapered shaft and the inertia of the disk on the first natural frequency of vibration for the system shown in Fig. 4.29

Table 4.2 Comparison of the first natural frequency results of the clamped support from left and right which can be seen in Fig. 4.27 and Fig. 4.29.

| | $I=0$ kg.m ² | $I=1$ kg.m ² | $I=2$ kg.m ² | $I=3$ kg.m ² | $I=4$ kg.m ² | $I=5$ kg.m ² | $I=10$ kg.m ² |
|--------------------|----------------------------|----------------------------|----------------------------|----------------------------|----------------------------|----------------------------|-----------------------------|
| Clamped from left | 1727.487 | 538.1137 | 389.9623 | 321.1058 | 279.2783 | 250.4406 | 178.013 |
| Clamped from right | 10011.999 | 565.5689 | 400.0335 | 326.6575 | 282.9073 | 253.0474 | 178.9419 |

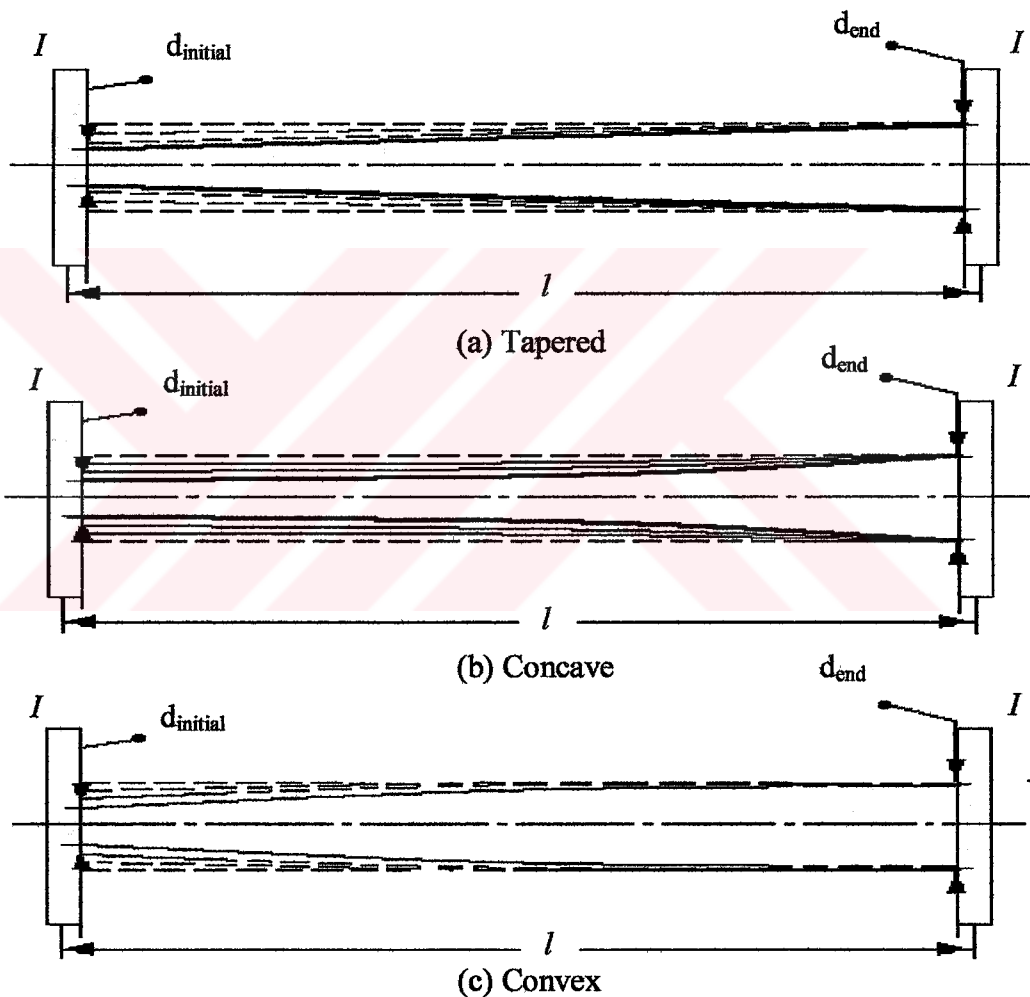


Figure 4.31 The multi disk-shaft systems having two discs and (a) tapered, (b) concave, (c) convex shaft with free-free support conditions.

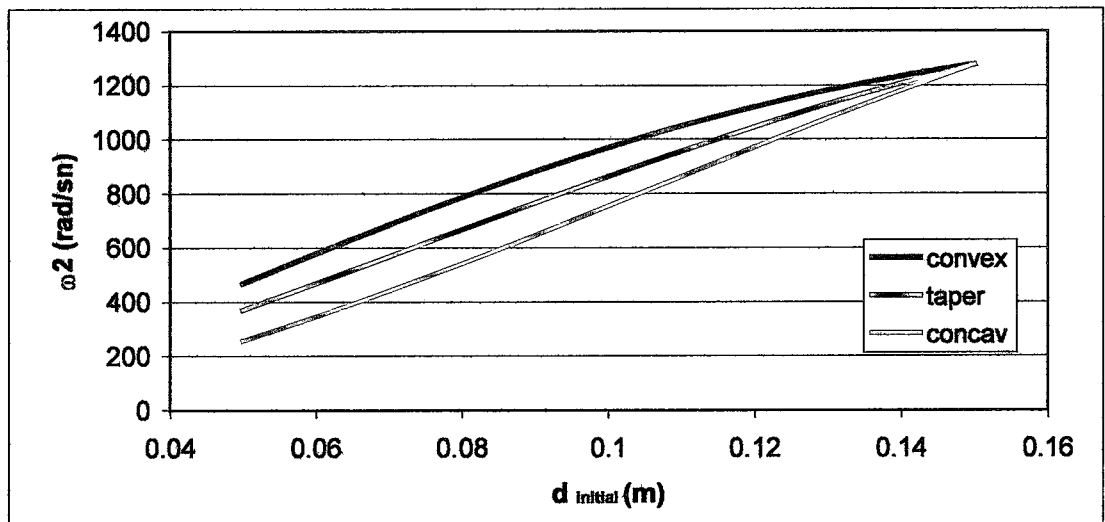


Figure 4.32 The effects of increasing the first diameter of convex, tapered and concave shaft on the first natural frequency for the systems shown in Fig. 4.31

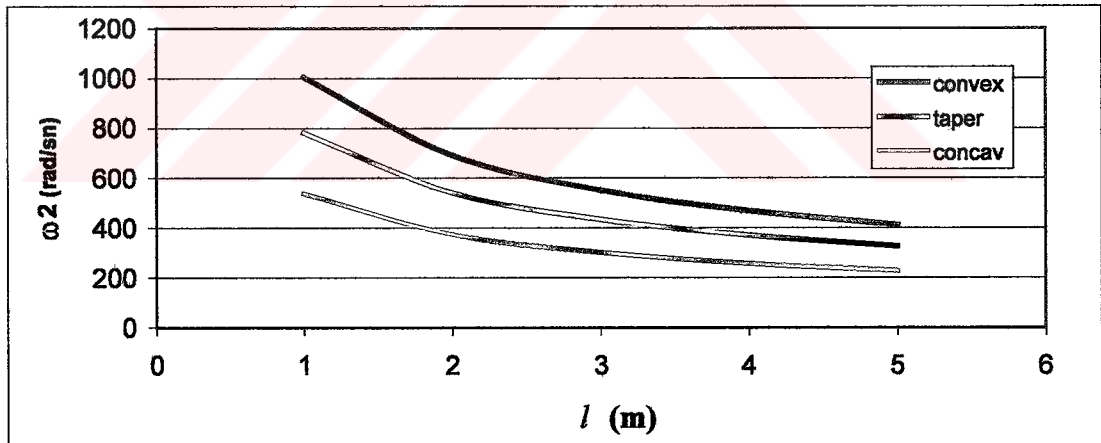


Figure 4.33 The effects of increasing the length of convex, tapered and concave shaft on the first natural frequency for the systems shown in Fig. 4.31

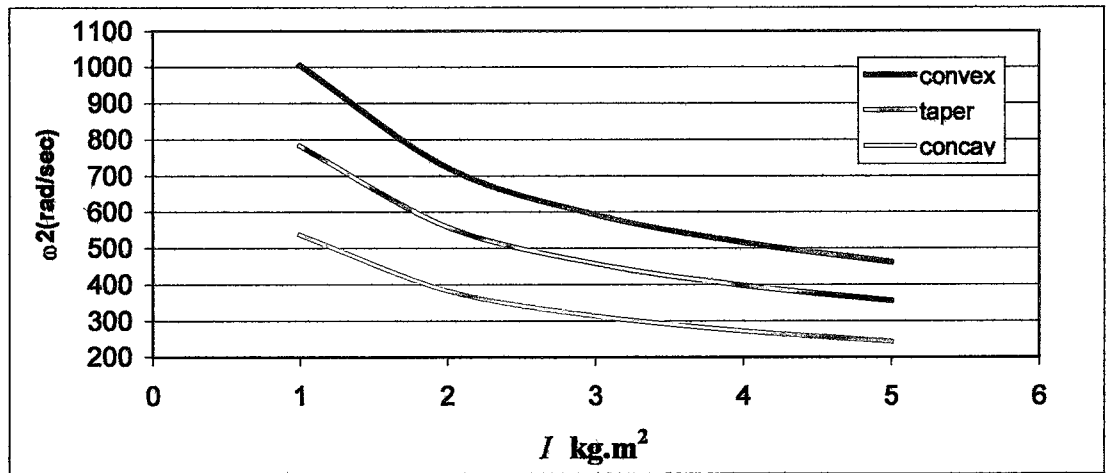


Figure 4.34 The effects of increasing the inertia of the discs on convex, tapered and concave shaft on the first natural frequency for the systems shown in Fig. 4.31

REFERENCES

- [1] PESTEL, C., & LECKIE, F. A. Matrix Methods in Elastomechanics. McGraw-Hill Book Company, Inc., New York, 1963.
- [2] CHANDRUPATLA, T. R. & BELEGUNDU, A. D. Introduction to Finite Elements in Engineering. Prentice Hall, Upper Saddle River, New Jersey, 1997.
- [3] ÖZGÜVEN, H. N. "On The Critical Speed of Continuous Shaft-Disk Systems," Journal of Vibration, Acoustics, Stress, and Reliability in Design, Vol.106, January 1984, pp 59-61.
- [4] KELLY, S. G. Mechanical Vibrations. McGraw-Hill, Inc., Singapore, 1993.
- [5] ÖZTÜRK, H. Effect of Spring Stiffness and Spring Position on the Dynamic Stability of Cantilever, Non-Uniform Cross-Sectioned, Timoshenko Beams Subjected to Periodic Axial Loading, Master Thesis, İzmir, Dokuz Eylül Üniversitesi, April, 1999.
- [6] KWON, Y. W., & BANG, H. The Finite Element Method Using MATLAB, CRC Press, New York, 1997.
- [7] MEIROVITCH, L. Elements of Vibration Analysis, McGraw-Hill, Inc., Tokyo, 1975.
- [8] KÖSER, K., PASİN, F. "Continuous Modeling of the Torsional Vibrations of the Drive Shaft of Mechanisms", Journal of Sound and Vibration, v188,n1, Nov 23, 1995 Academic Press Ltd, London, England, p 17-24.
- [9] PETYT. M. Introduction to Finite Element Vibration Analysis, Cambridge University Press, Cambridge, 1990.

- [10] KANEKO, Y., MOMOO, T., OKADA, Y. "Torsional Vibration Analysis of Blade-Disk-Shaft System by the Finite Element Method and the Transfer Matrix Method", Transactions of the Japan Society Mechanical Engineers, Part C, v61, n586, Jun, 1995 JSME, Tokyo, Japan, p 36-41.
- [11] KATO, M., OTA, H., NAKAMURA, S. "Torsional Vibration of a Rotating Shaft in Passing Through the Critical Speed of Whirling Vibration", Transactions of the Japan Society Mechanical Engineers, Part C, v61, n584, Apr, 1995 JSME, Tokyo, Japan, p 1265-1270.
- [12] GÜNEŞ, A., & YILDIZ, K. MATLAB for Windows, Türkmen Kitabevi, İstanbul, 1997.
- [13] YÜKSEL, İ. MATLAB ile Mühendislik Sistemlerinin Analizi ve Çözümü, Bursa, Uludağ Üniversitesi, 1996





APPENDIX

```

Private Sub atalet_etikisi_Click()
Cls
Open "c:\saha\tez\ataletetikisi1.txt" For Output As 1
Open "c:\saha\tez\ataletetikisi.xls" For Output As 2
n = 2
ReDim rigit(n - 1), atalet(n), K12(n - 1), M21(n), a(n), b(n)
'-----
ilkatalet = 1
sonatalet = 100
aralik = (sonatalet - ilkatalet)
For v = ilkatalet To sonatalet
f = 1000000
'-----
'-----
For i = 1 To n
atalet(i) = v
Next i
For i = 1 To (n - 1)
rigit(i) = f
Next i

'-----
M11 = 1
M12 = 0
M22 = 1
K11 = 1
K21 = 0
K22 = 1
'-----

'-----birinci dogal frekansin bulunmasi-----
wilk = 1
wson = 5000 * wilk
kat = 2
hassasiyet = 0.0001

GoTo 50

30 wilk = w - kat
wson = w
kat = kat / 10

50 For i = wilk To wson Step kat

```

```

For J = 1 To (n - 1)
K12(J) = 1 / rigit(J)
Next J
For J = 1 To n
M21(J) = -i ^ 2 * atalet(J)
Next J

a(1) = K11 * M11 + K12(1) * M21(1)
b(1) = K21 * M11 + K22 * M21(1) + M21(2) * a(1)
If n = 2 Then GoTo 55
For s = 1 To n - 2
  a(s + 1) = K11 * a(s) + K12(s + 1) * b(s)
  b(s + 1) = K21 * a(s) + K22 * b(s) + M21(s + 2) * a(s + 1)
Next s

55 w = i
If kat <= hassasiyet Then GoTo 80
If pes * b(n - 1) < 0 Then GoTo 30
pes = b(n - 1)
Next i
80 Print #1, v, w - kat
Print #2, v, w - kat
Print

Next v
Close #1
Close #2
Open "c:\saha\tez\ataletetkisi1.txt" For Input As 1
ny = aralik
ReDim X(ny), Y(ny)

For i = 1 To ny
Input #1, X(i), Y(i)
Next i
Close #1

  ymin = Y(1): ymax = Y(1)
  For i = 2 To ny
    If Y(i) > ymax Then ymax = Y(i)
    If Y(i) < ymin Then ymin = Y(i)
  Next i
  If ymax = ymin Then ymax = ymax + 1: ymin = ymin - 1

Picture1.Scale (1, ymax)-(ny, ymin)
Picture1.PSet (1, Y(1)), c

```



```

For i = 2 To ny
For J = 1 To 10000
Next J
Picture1.Line -(i, Y(i)), RGB(Rnd * 800, 0, 0)
Next i

```

```
End Sub
```

```

n = 2
ReDim right(n - 1), atalet(n), K12(n - 1), M21(n), a(n), b(n), a2(n), b2(n)

```

```

'-----
E = 2.1 * 10 ^ 11
nu = 0.26
G = E / (2 * (1 + nu))
pi = 3.141596
d1 = 0.1
d2 = 0.1
l1 = 4
l2 = 4

```

```

'-----
J1 = pi * d1 ^ 4 / 32
J2 = pi * d1 ^ 4 / 32
kcof1 = G * J1 / l1
kcof2 = G * J2 / l2

```

```

v = 1.13
f1 = kcof1
f2 = kcof2
For i = 1 To n
atalet(i) = v
Next i

```

```

For i = 1 To n - 1
right(i) = f1
Next i

```

```

'-----
M11 = 1
M12 = 0
M22 = 1
K11 = 1
K21 = 0
K22 = 1

```

```

'-----
'-----birinci dogal frekansin bulunmasi-----
wilk = 1
wson = 5000 * wilk
kat = 10
hassasiyet = 0.0000001

GoTo 50

30 wilk = w - kat
wson = w
kat = kat / 10

50 For i = wilk To wson Step kat
For J = 1 To (n - 1)
K12(J) = 1 / rigit(J)
Next J
For J = 1 To n
M21(J) = -i ^ 2 * atalet(J)
Next J

a(1) = K11 * M11 + K12(1) * M21(1)
b(1) = K21 * M11 + K22 * M21(1) + M21(2) * a(1)
If n = 2 Then GoTo 55
For s = 1 To n - 2
a(s + 1) = K11 * a(s) + K12(s + 1) * b(s)
b(s + 1) = K21 * a(s) + K22 * b(s) + M21(s + 2) * a(s + 1)
Next s

55 w = i
If kat <= hassasiyet Then GoTo 80
If pes * b(n - 1) < 0 Then GoTo 30
pes = b(n - 1)
Next i
80 Print "rigitlik="; f,
Print "1. dogal frekans="; w - kat
dogfre1.Text = Str$(w - kat)

'-----ikinci dog fre-----
wilk = w + 20
wson = wilk * 100
kat = 10

```

```
hassasiyet = 0.0000001
GoTo 52
```

```
32 wilk = w - kat
wson = w
kat = kat / 10
```

```
52 For i = wilk To wson Step kat
For J = 1 To (n - 1)
K12(J) = 1 / rigit(J)
Next J
For J = 1 To n
M21(J) = -i ^ 2 * atalet(J)
Next J
```

```
a2(1) = K11 * M11 + K12(1) * M21(1)
b2(1) = K21 * M11 + K22 * M21(1) + M21(2) * a2(1)
If n = 2 Then GoTo 552
For s = 1 To n - 2
a2(s + 1) = K11 * a2(s) + K12(s + 1) * b2(s)
b2(s + 1) = K21 * a2(s) + K22 * b2(s) + M21(s + 2) * a2(s + 1)
Next s
552 w = i
If kat <= hassasiyet Then GoTo 82
If pes2 * b2(n - 1) < 0 Then GoTo 32
pes2 = b2(n - 1)
Next i
82 Print "rigitlik="; f,
Print "2. dogal frekans="; w - kat
dogfre2.Text = Str$(w - kat)
End Sub
```

```
% Natural Frequency Analysis for Clamped-Clamped Support
```

```
E=2.1*10^11;%(N/m^2)
nu=0.26;
G=E/(2*(1+nu));
pi=3.141596;
ro=7800;%(kg/m^3)
%-----
Is=zeros;
```

```

L=zeros;
le=zeros;
d=zeros;
J=zeros;
mcof=zeros;
kcof=zeros;

N=input('enter the number of disks=')

for i=1:N
    Is(i)=input('enter the inertia of disks (kg.m^2)=')
end

for i=1:N-1
    L(i)=input('enter the length of shaft segments (m)=')
    end
    for i=1:N-1
        d(i)=input('enter the diameter of shaft segments (m)=')
    end
    for i=1:N-1
        J(i)=pi*(d(i))^4/32;
    end
    n=input('enter the number of divide of the shaft segments=')
    for i=1:N-1
        le(i)=L(i)/n;
        kcof(i)=G*J(i)/le(i)
        mcof(i)=ro*J(i)*le(i)/6;
    end
    %-----
    k=[1,-1:-1,1];
    m=[2,1:1,2];
    %-----
    kgenel=zeros(n*(N-1)+1);
    mgenel=zeros(n*(N-1)+1);
    kgenelx=zeros(n*(N-1)+1);
    mgenelx=zeros(n*(N-1)+1);

    for i=1:(n*(N-1))
        kgenel(i,i+1)=-1;
        kgenel(i+1,i)=-1;
    end

    kgenel(1,1)=1;
    kgenel(n*(N-1)+1,n*(N-1)+1)=1;

```

```

for i=2:(n*(N-1));
    kgenel(i,i)=2;
end;
%-----

for i=1:(n*(N-1));
    mgenel(i,i+1)=1;
    mgenel(i+1,i)=1;
end;

mgenel(1,1)=2;
mgenel(n*(N-1)+1,n*(N-1)+1)=2;

for i=2:(n*(N-1));
    mgenel(i,i)=4;
end;
kgenel;
mgenel;
%-----
%-----

a=1;
for j=1:N-1;
    for i=a:n+a-1;
        kgenelx(i,i)=kgenel(i,i)*kcof(j);
        kgenelx(i,i+1)=kgenel(i,i+1)*kcof(j);
        kgenelx(i+1,i)=kgenel(i+1,i)*kcof(j);
        mgenelx(i,i)=mgenel(i,i)*mcof(j);
        mgenelx(i,i+1)=mgenel(i,i+1)*mcof(j);
        mgenelx(i+1,i)=mgenel(i+1,i)*mcof(j);

    end;
    a=a+n;
end;
j=1;
for i=n+1:n*(N-2)+1;
    kgenelx(i,i)=1*(kcof(j)+kcof(j+1));
    mgenelx(i,i)=2*(mcof(j)+mcof(j+1));
    j=j+1;
end;
format long
kgenelx(n*(N-1)+1,n*(N-1)+1)=kgenel(n*(N-1)+1,n*(N-1)+1)*kcof(N-1);
mgenelx(n*(N-1)+1,n*(N-1)+1)=mgenel(n*(N-1)+1,n*(N-1)+1)*mcof(N-1);
q=1;
for i=1:n:(n*(N-1)+1);

```

```

    mgenelx(i,i)=mgenelx(i,i)+Is(q);
    q=q+1;
end
kcof(1);

```

```

mcof(1);
kgenelx
mgenelx
format long
kgenelx(1,:)=[];
kgenelx(:,1)=[];
mgenelx(1,:)=[];
mgenelx(:,1)=[];
kgenelx(n*(N-1),:)=[];
kgenelx(:,n*(N-1))=[];
mgenelx(n*(N-1),:)=[];
mgenelx(:,n*(N-1))=[];

```

```

A=sort(eig(kgenelx,mgenelx));
w=sqrt(A)
w(A)

```

```

% Natural Frequency Analysis for Clamped-Free Support

```

```

E=2.1*10^11;%(N/m^2)
nu=0.26;
G=E/(2*(1+nu));
pi=3.141596;
ro=7800;%(kg/m^3)
%-----

```

```

Is=zeros;
L=zeros;
le=zeros;
d=zeros;
J=zeros;
mcof=zeros;
kcof=zeros;

```

```

N=input('enter the number of disks=')

```

```

for i=1:N
    Is(i)=input('enter the inertia of disks (kg.m^2)=')

```

```

end

for i=1:N-1
    L(i)=input('enter the length of shaft segments (m)=')
end
for i=1:N-1
    d(i)=input('enter the diameter of shaft segments (m)=')
end
for i=1:N-1
    J(i)=pi*(d(i))^4/32;
end
n=1;input('enter the number of divide of the shaft segments=')
for i=1:N-1
    le(i)=L(i)/n;
    kcof(i)=G*J(i)/le(i)
    mcof(i)=ro*J(i)*le(i)/6;
end
%-----
k=[1,-1:-1,1];
m=[2,1:1,2];
%-----
kgenel=zeros(n*(N-1)+1);
mgenel=zeros(n*(N-1)+1);
kgenelx=zeros(n*(N-1)+1);
mgenelx=zeros(n*(N-1)+1);

for i=1:(n*(N-1))
    kgenel(i,i+1)=-1;
    kgenel(i+1,i)=-1;
end

kgenel(1,1)=1;
kgenel(n*(N-1)+1,n*(N-1)+1)=1;

for i=2:(n*(N-1));
    kgenel(i,i)=2;
end;
%-----

for i=1:(n*(N-1));
    mgenel(i,i+1)=1;
    mgenel(i+1,i)=1;
end;

mgenel(1,1)=2;

```

```

mgenel(n*(N-1)+1,n*(N-1)+1)=2;

for i=2:(n*(N-1));
    mgenel(i,i)=4;
end;
kgenel;
mgenel;
%-----
%-----

a=1;
for j=1:N-1;
    for i=a:n+a-1;
        kgenelx(i,i)=kgenel(i,i)*kcof(j);
        kgenelx(i,i+1)=kgenel(i,i+1)*kcof(j);
        kgenelx(i+1,i)=kgenel(i+1,i)*kcof(j);
        mgenelx(i,i)=mgenel(i,i)*mcof(j);
        mgenelx(i,i+1)=mgenel(i,i+1)*mcof(j);
        mgenelx(i+1,i)=mgenel(i+1,i)*mcof(j);
    end;
    a=a+n;
end;
j=1;
for i=n+1:n*(N-2)+1;
    kgenelx(i,i)=1*(kcof(j)+kcof(j+1));
    mgenelx(i,i)=2*(mcof(j)+mcof(j+1));
    j=j+1;
end;
format long
kgenelx(n*(N-1)+1,n*(N-1)+1)=kgenel(n*(N-1)+1,n*(N-1)+1)*kcof(N-1);
mgenelx(n*(N-1)+1,n*(N-1)+1)=mgenel(n*(N-1)+1,n*(N-1)+1)*mcof(N-1);
q=1;
for i=1:n*(N-1)+1;
    mgenelx(i,i)=mgenelx(i,i)+Is(q);
    q=q+1;
end
kcof(1);

mcof(1);
kgenelx
mgenelx
format long
kgenelx(1,:)=[];
kgenelx(:,1)=[];

```



```
mgenelx(1,:)=[];
mgenelx(:,1)=[];
```

```
A=sort(eig(kgenelx,mgenelx));
w=sqrt(A)
w(A)
```

```
% Natural Frequency Analysis for Free-Free Support
```

```
E=2.1*10^11;%(N/m^2)
```

```
nu=0.26;
```

```
G=E/(2*(1+nu));
```

```
pi=3.141596;
```

```
ro=7800;%(kg/m^3)
```

```
%-----
```

```
Is=zeros;
```

```
L=zeros;
```

```
le=zeros;
```

```
d=zeros;
```

```
J=zeros;
```

```
mcof=zeros;
```

```
kcof=zeros;
```

```
N=input('enter the number of disks=')
```

```
for i=1:N
```

```
    Is(i)=input('enter the inertia of disks (kg.m^2)=')
```

```
end
```

```
for i=1:N-1
```

```
    L(i)=input('enter the length of shaft segments (m)=')
```

```
    end
```

```
    for i=1:N-1
```

```
        d(i)=input('enter the diameter of shaft segments (m)=')
```

```
    end
```

```
for i=1:N-1
```

```
    J(i)=pi*(d(i))^4/32;
```

```
end
```

```
n=1;input('enter the number of divide of the shaft segments=')
```

```
for i=1:N-1
```

```
    le(i)=L(i)/n;
```

```
    kcof(i)=G*J(i)/le(i)
```

```

    mcoff(i)=ro*J(i)*le(i)/6;
end
%-----
k=[1,-1:-1,1];
m=[2,1:1,2];
%-----
kgenel=zeros(n*(N-1)+1);
mgenel=zeros(n*(N-1)+1);
kgenelx=zeros(n*(N-1)+1);
mgenelx=zeros(n*(N-1)+1);

for i=1:(n*(N-1))
    kgenel(i,i+1)=-1;
    kgenel(i+1,i)=-1;
end

kgenel(1,1)=1;
kgenel(n*(N-1)+1,n*(N-1)+1)=1;

for i=2:(n*(N-1));
    kgenel(i,i)=2;
end;
%-----

for i=1:(n*(N-1));
    mgenel(i,i+1)=1;
    mgenel(i+1,i)=1;
end;

mgenel(1,1)=2;
mgenel(n*(N-1)+1,n*(N-1)+1)=2;

for i=2:(n*(N-1));
    mgenel(i,i)=4;
end;
kgenel;
mgenel;
%-----
%-----

a=1;
for j=1:N-1;
    for i=a:n+a-1;
        kgenelx(i,i)=kgenel(i,i)*kcoff(j);
        kgenelx(i,i+1)=kgenel(i,i+1)*kcoff(j);
    end
end

```

```

kgenelx(i+1,i)=kgenel(i+1,i)*kcof(j);
mgenelx(i,i)=mgenel(i,i)*mcof(j);
mgenelx(i,i+1)=mgenel(i,i+1)*mcof(j);
mgenelx(i+1,i)=mgenel(i+1,i)*mcof(j);

end;
a=a+n;
end;
j=1;
for i=n+1:n*(n)*(N-2)+1;
    kgenelx(i,i)=1*(kcof(j)+kcof(j+1));
    mgenelx(i,i)=2*(mcof(j)+mcof(j+1));
    j=j+1;
end;
format long
kgenelx(n*(N-1)+1,n*(N-1)+1)=kgenel(n*(N-1)+1,n*(N-1)+1)*kcof(N-1);
mgenelx(n*(N-1)+1,n*(N-1)+1)=mgenel(n*(N-1)+1,n*(N-1)+1)*mcof(N-1);
q=1;
for i=1:n*(n*(N-1)+1);
    mgenelx(i,i)=mgenelx(i,i)+Is(q);
    q=q+1;
end
kcof(1);

mcof(1);
kgenelx
mgenelx
format long

A=sort(eig(kgenelx,mgenelx));
w=sqrt(A)
w(A)

```

%The Natural Frequency Analysis for the Concav Shaft

```

E=2.1*10^11;%(N/m^2)
nu=0.26;
G=E/(2*(1+nu));
pi=3.141596;
ro=7800;%(kg/m^3)
%-----
Is=zeros;

```

```

L=zeros;
d=zeros;
J=zeros;
x=zeros;
dq=zeros;
%-----

n=4;

d=zeros(n);

dilk=input('enter the inertial diameter of the concav shaft=')
dson=input('enter the end diameter of the concav shaft=')
Is(1)=input('enter the inertia of the first disk=')
Is(2)=input('enter the inertia of the second disk=')
L=input('enter the length of the shaft=')
xb=L/n;
dq(1)=dilk
dq(n+1)=dson
for i=2:n
dq(i)=(dilk+((dson-dilk)/L^2)*(xb*(i-1))^2);
end
for i=1:n
    d(i)=(dq(i)+dq(i+1))/2;
end
for i=1:n
    J(i)=pi*(d(i))^4/32;
end
for i=1:n
    kcof(i)=G*J(i)/xb;
    mcof(i)=ro*J(i)*xb/6;
end

%-----
k=[1,-1:-1,1];
m=[2,1:1,2];
%-----
kgenel=zeros(n+1);
mgenel=zeros(n+1);
kgenelx=zeros(n+1);
mgenelx=zeros(n+1);

for i=1:(n+1)
    kgenel(i,i+1)=-1;
    kgenel(i+1,i)=-1;

```

```

    kgenel(i,i)=1;
end
for i=1:(n+1)
    mgenel(i,i+1)=1;
    mgenel(i+1,i)=1;
    mgenel(i,i)=2;
end

%-----
kgenelx(1,1)=kgenel(1,1)+kcof(1);
kgenelx(n+1,n+1)=kgenel(n+1,n+1)+kcof(n);

for i=2:n
    kgenelx(i,i)=kgenel(i,i)*(kcof(i-1)+kcof(i));
end
for i=1:n
    kgenelx(i,i+1)=kgenel(i,i+1)*kcof(i);
    kgenelx(i+1,i)=kgenel(i+1,i)*kcof(i);
end

mgenelx(1,1)=mgenel(1,1)*mcof(1);
mgenelx(n+1,n+1)=mgenel(n+1,n+1)*mcof(n);

for i=2:n
    mgenelx(i,i)=mgenel(i,i)*(mcof(i-1)+mcof(i));
end
for i=1:n
    mgenelx(i,i+1)=mgenel(i,i+1)*mcof(i);
    mgenelx(i+1,i)=mgenel(i+1,i)*mcof(i);
end

mgenelx(1,1)=mgenelx(1,1)+Is(1);
mgenelx(n+1,n+1)=mgenelx(n+1,n+1)+Is(2);
kgenelx;
mgenelx;

format long
A=sort(eig(kgenelx,mgenelx));
w=sqrt(A)

```

%The Natural Frequency Analysis for the Convex Shaft

```

E=2.1*10^11;%(N/m^2)
nu=0.26;
G=E/(2*(1+nu));
pi=3.141596;
ro=7800;%(kg/m^3)
%-----
Is=zeros;
L=zeros;
d=zeros;
J=zeros;
x=zeros;
dq=zeros;
%-----

n=4;

d=zeros(n);

dilk=input('enter the inertial diameter of the convex shaft=')
dson=input('enter the end diameter of the convex shaft=')
Is(1)=input('enter the inertia of the first disk=')
Is(2)=input('enter the inertia of the second disk=')
L=input('enter the length of the shaft=')
xb=L/n;
dq(1)=dilk
dq(n+1)=dson
for i=2:n
dq(i)=dilk+2*(dson-dilk)*xb*(i-1)/L-(dson-dilk)*(xb*(i-1)/L)^2;
end
for i=1:n
    d(i)=(dq(i)+dq(i+1))/2;
end
for i=1:n
    J(i)=pi*(d(i))^4/32;
end
for i=1:n
    kcof(i)=G*J(i)/xb;
    mcof(i)=ro*J(i)*xb/6;
end

%-----
k=[1,-1:-1,1];

```

```

m=[2,1:1,2];
%-----
mgenel=zeros(n+1);
mgenel=zeros(n+1);
kgenelx=zeros(n+1);
mgenelx=zeros(n+1);

for i=1:(n+1)
    kgenel(i,i+1)=-1;
    kgenel(i+1,i)=-1;
    kgenel(i,i)=1;
end
for i=1:(n+1)
    mgenel(i,i+1)=1;
    mgenel(i+1,i)=1;
    mgenel(i,i)=2;
end

%-----
kgenelx(1,1)=kgenel(1,1)+kcof(1);
kgenelx(n+1,n+1)=kgenel(n+1,n+1)+kcof(n);

for i=2:n
    kgenelx(i,i)=kgenel(i,i)*(kcof(i-1)+kcof(i));
end
for i=1:n
    kgenelx(i,i+1)=kgenel(i,i+1)*kcof(i);
    kgenelx(i+1,i)=kgenel(i+1,i)*kcof(i);
end

mgenelx(1,1)=mgenel(1,1)*mcof(1);
mgenelx(n+1,n+1)=mgenel(n+1,n+1)*mcof(n);

for i=2:n
    mgenelx(i,i)=mgenel(i,i)*(mcof(i-1)+mcof(i));
end
for i=1:n
    mgenelx(i,i+1)=mgenel(i,i+1)*mcof(i);
    mgenelx(i+1,i)=mgenel(i+1,i)*mcof(i);
end

mgenelx(1,1)=mgenelx(1,1)+Is(1);
mgenelx(n+1,n+1)=mgenelx(n+1,n+1)+Is(2);
kgenelx;
mgenelx;

```

```
format long
A=sort(eig(kgenelx,mgenelx));
w=sqrt(A)
```

```
%The Natural Frequency Analysis for the Tapered Shaft
```

```
E=2.1*10^11;%(N/m^2)
nu=0.26;
G=E/(2*(1+nu));
pi=3.141596;
ro=7800;%(kg/m^3)
%-----
Is=zeros;
L=zeros;
d=zeros;
J=zeros;
x=zeros;
%-----

n=5;

d=zeros(n);

dilk=input('enter the inertial diameter of the convex shaft=')
dson=input('enter the end diameter of the convex shaft=')
Is(1)=input('enter the inertia of the first disk=')
Is(2)=input('enter the inertia of the second disk=')
L=input('enter the length of the shaft=')
xb=L/n;
dq=((dson-dilk)*xb/L)+dilk
d(1)=(dilk+dq)/2
for i=2:n
    d(i)=d(i-1)+(dson-dilk)*xb/L
end
for i=1:n
    J(i)=pi*(d(i))^4/32;
end
for i=1:n
    kcof(i)=G*J(i)/xb
    mcof(i)=ro*J(i)*xb/6;
```



```

end

%-----
k=[1,-1:-1,1];
m=[2,1:1,2];
%-----
kgenel=zeros(n+1);
mgenel=zeros(n+1);
kgenelx=zeros(n+1);
mgenelx=zeros(n+1);

for i=1:(n+1)
    kgenel(i,i+1)=-1;
    kgenel(i+1,i)=-1;
    kgenel(i,i)=1;
end
for i=1:(n+1)
    mgenel(i,i+1)=1;
    mgenel(i+1,i)=1;
    mgenel(i,i)=2;
end

%-----
kgenelx(1,1)=kgenel(1,1)+kcof(1);
kgenelx(n+1,n+1)=kgenel(n+1,n+1)+kcof(n);

for i=2:n
    kgenelx(i,i)=kgenel(i,i)*(kcof(i-1)+kcof(i));
end
for i=1:n
    kgenelx(i,i+1)=kgenel(i,i+1)*kcof(i);
    kgenelx(i+1,i)=kgenel(i+1,i)*kcof(i);
end

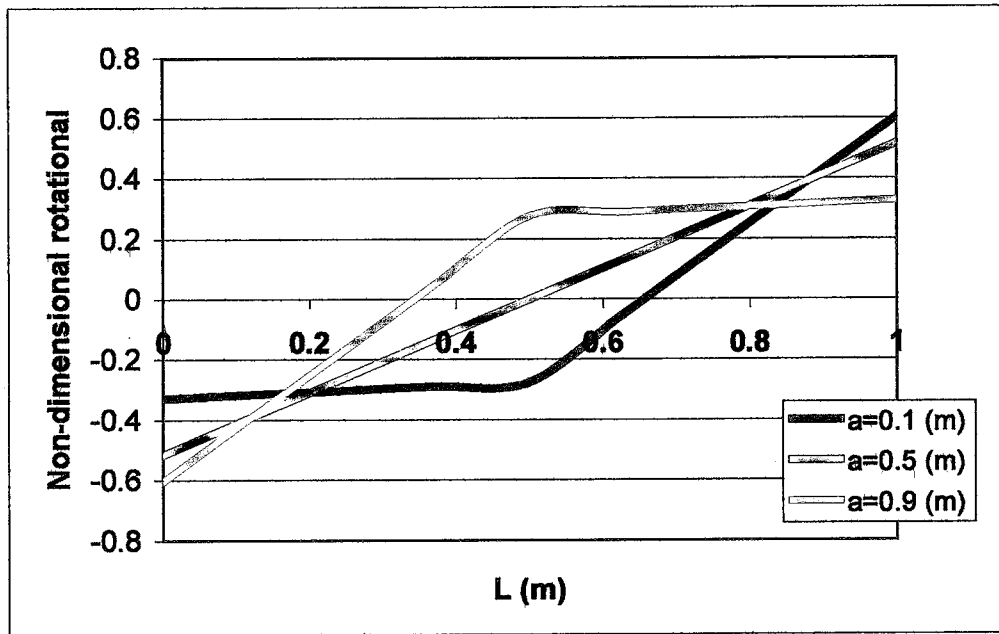
mgenelx(1,1)=mgenel(1,1)*mcof(1);
mgenelx(n+1,n+1)=mgenel(n+1,n+1)*mcof(n);

for i=2:n
    mgenelx(i,i)=mgenel(i,i)*(mcof(i-1)+mcof(i));
end
for i=1:n
    mgenelx(i,i+1)=mgenel(i,i+1)*mcof(i);
    mgenelx(i+1,i)=mgenel(i+1,i)*mcof(i);
end

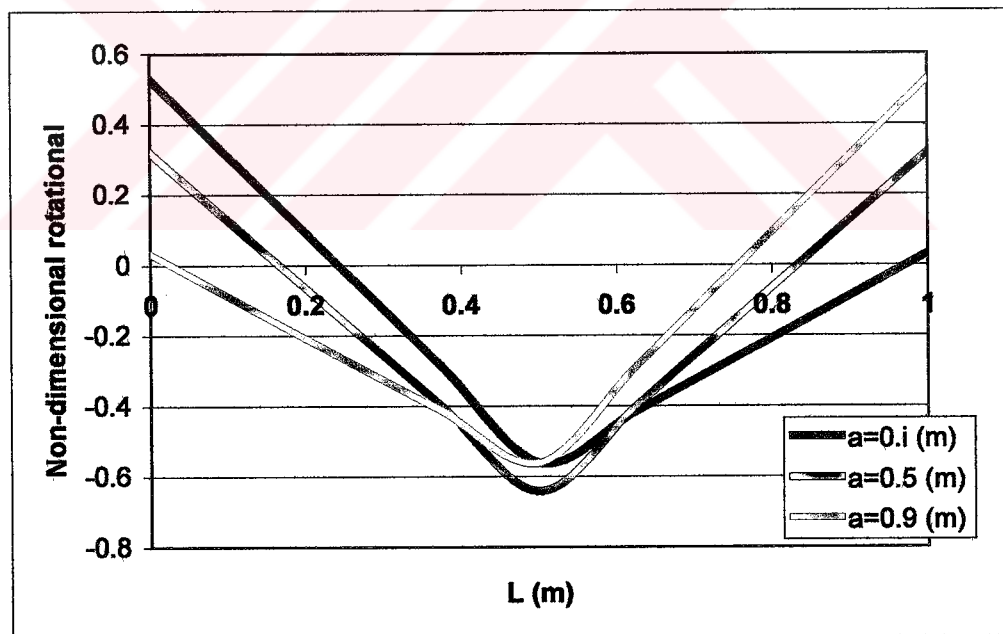
```

```
mgenelx(1,1)=mgenelx(1,1)+Is(1);  
mgenelx(n+1,n+1)=mgenelx(n+1,n+1)+Is(2);  
kgenelx  
mgenelx  
  
format long  
A=sort(eig(kgenelx,mgenelx));  
w=sqrt(A)
```

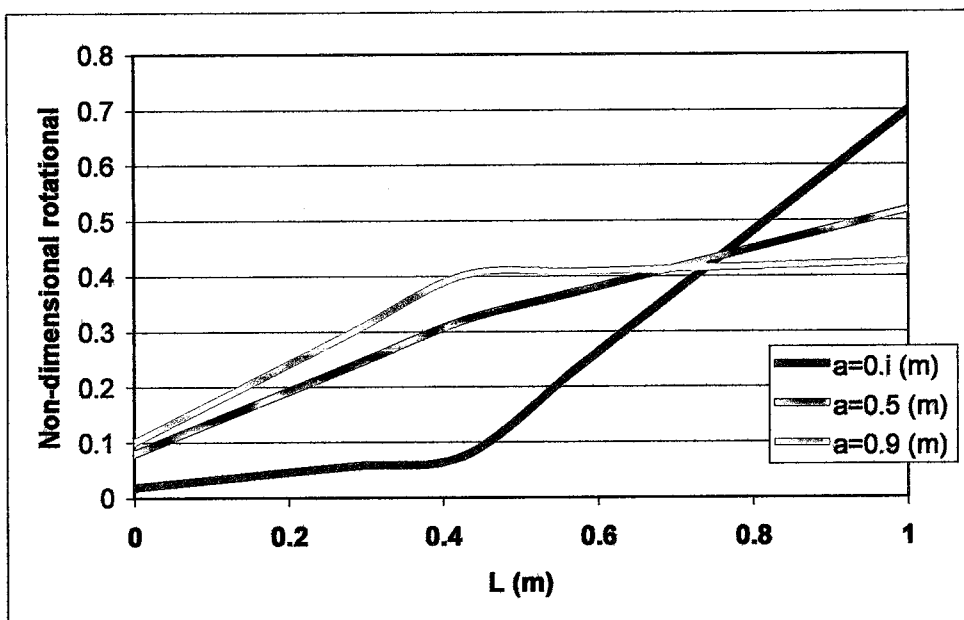




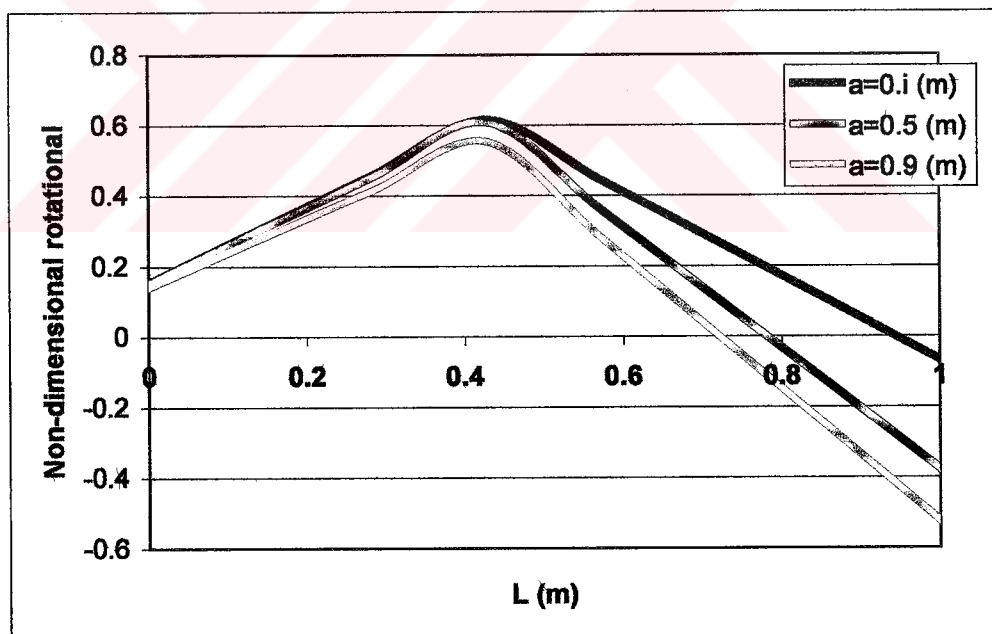
The mode shape of first natural frequency for the system of given in Fig. 4.7



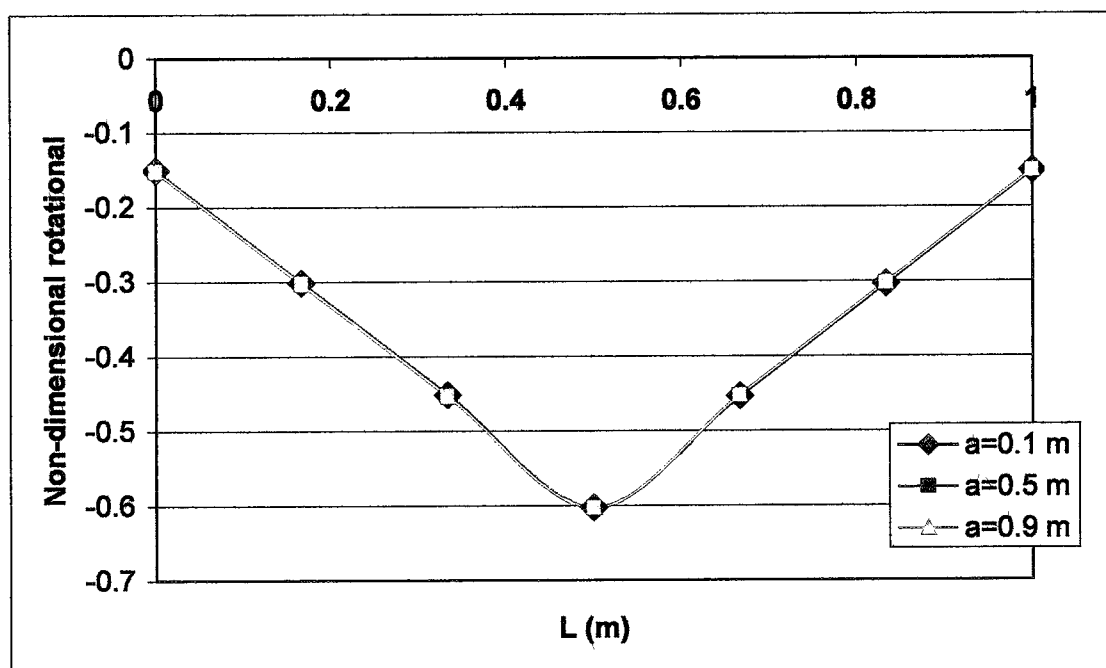
The mode shape of second natural frequency for the system of given in Fig. 4.7



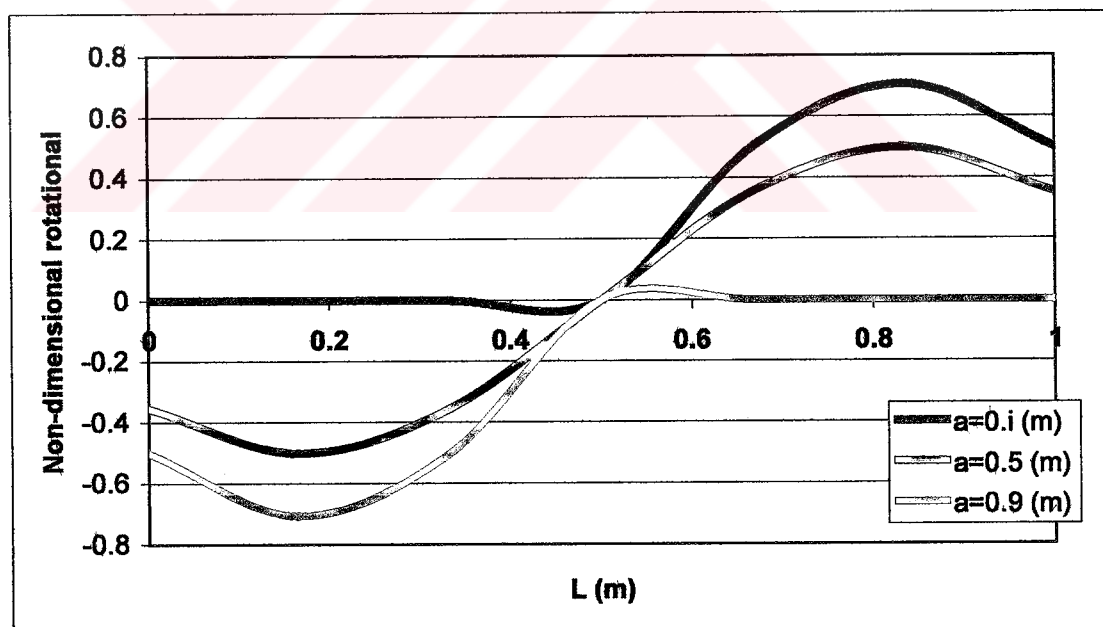
The mode shape of first natural frequency for the system of given in Fig. 4.10



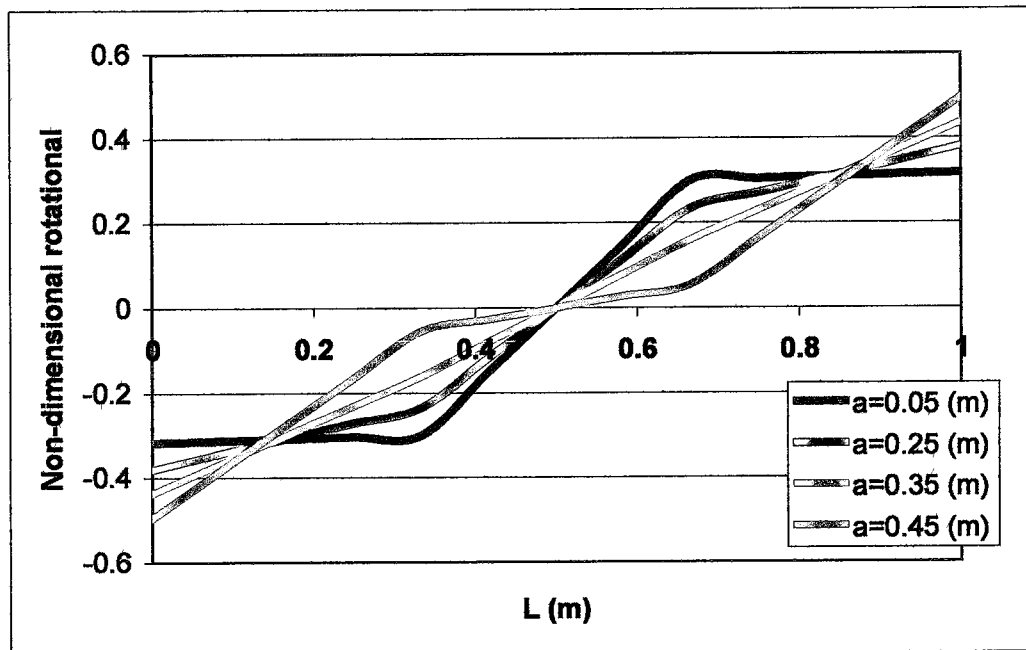
The mode shape of second natural frequency for the system of given in Fig. 4.10



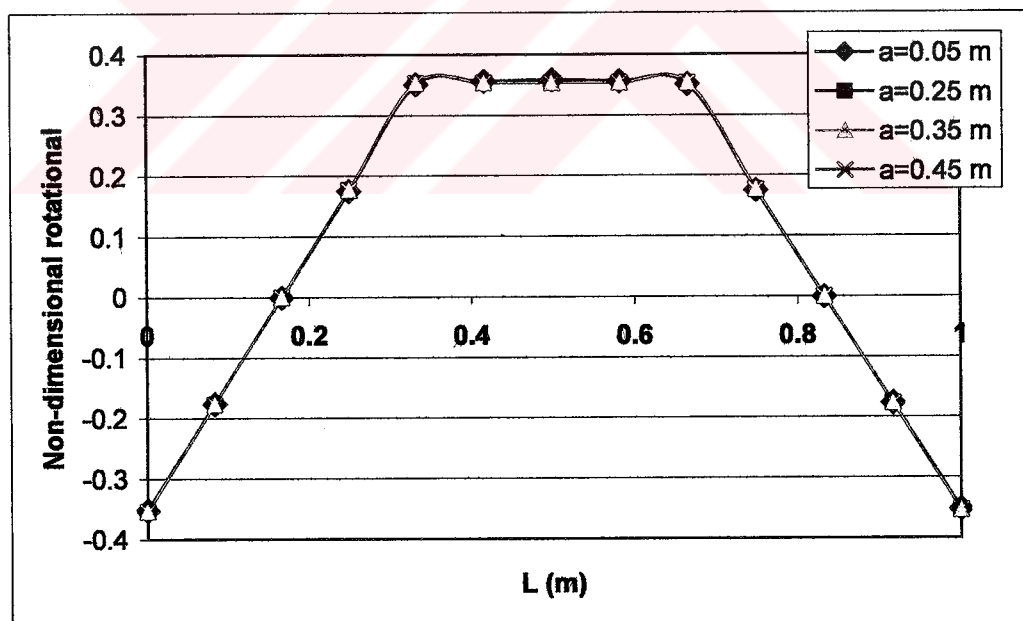
The mode shape of first natural frequency for the system of given in Fig. 4.13



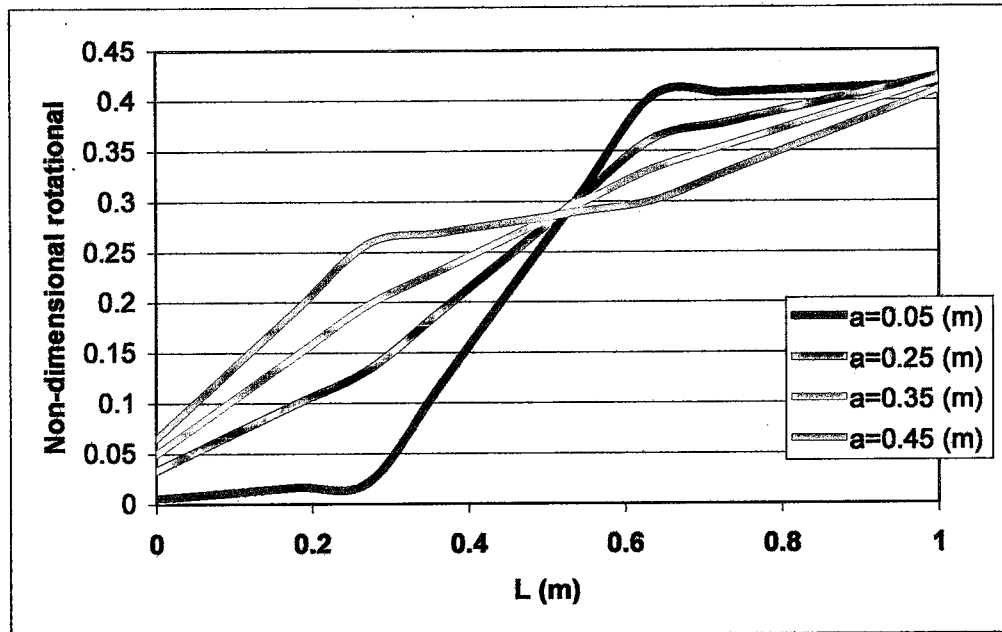
The mode shape of second natural frequency for the system of given in Fig. 4.13



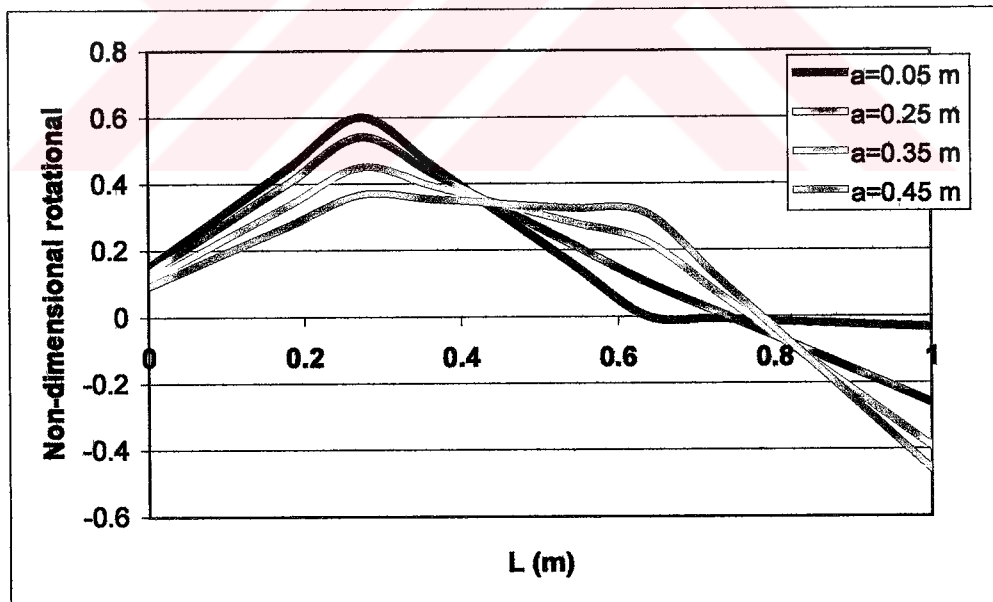
The mode shape of first natural frequency for the system of given in Fig. 4.16



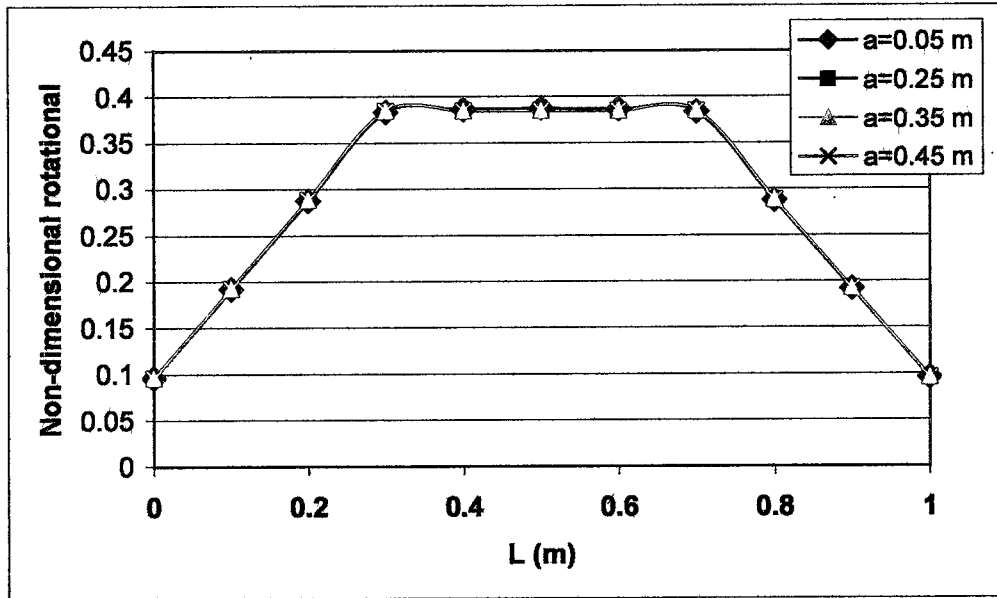
The mode shape of second natural frequency for the system of given in Fig. 4.16



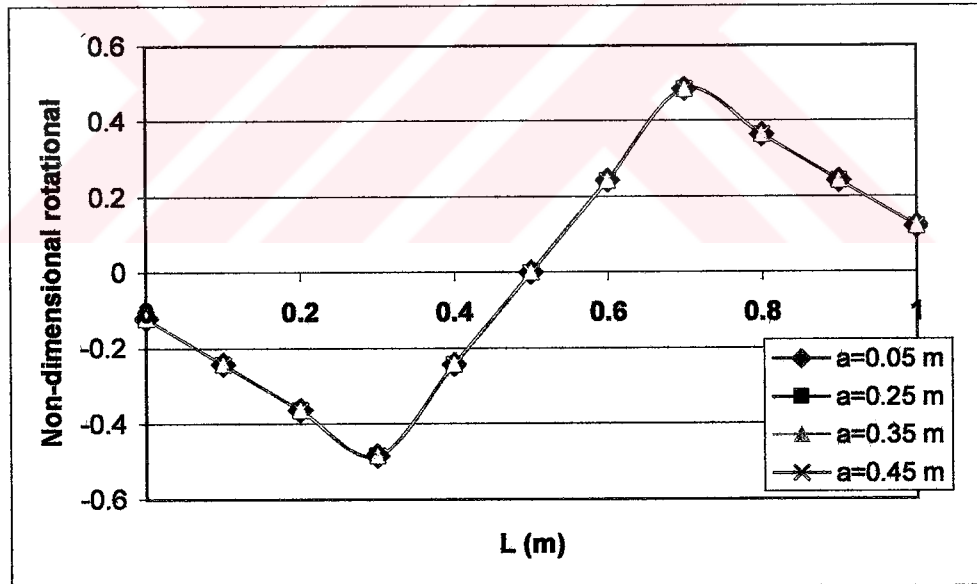
The mode shape of first natural frequency for the system of given in Fig. 4.19



The mode shape of second natural frequency for the system of given in Fig. 4.19



The mode shape of first natural frequency for the system of given in Fig. 4.22



The mode shape of second natural frequency for the system of given in Fig. 4.22